

MITIGATING FREEZE-THAW DAMAGE IN SOILS VIA PHASE CHANGE MATERIALS
(PCM)

By

Berkay Azakli

A THESIS

Submitted to
Michigan State University
in partial fulfillment of the requirements
for the degree of

Civil Engineering-Master of Science

2024

ABSTRACT

Freeze-thaw (F-T) cycles cause significant frost heaving and thaw weakening in roadway subgrade soils. Frost heaving and thaw weakening occur only when there is available water, frost susceptible soil and temperature fluctuations around the freezing temperature of water. The goal of this study is to use Phase Change Materials (PCMs) to lower freezing temperature of soils and minimize the temperature fluctuations during F-T cycles. PCMs absorb and/or release high latent heat when they undergo a phase change. PCMs with the appropriate phase change temperature have the potential to reduce temperature fluctuations around the freezing/thawing point of soil, thereby helping reduce the damage inflicted by freeze-thaw cycles.

In this study, three different types of PCMs were mixed with Glacial Till (GT) and Sandy Soil (SS). The PCM types were inorganic PCM (PCM-A), organic PCM (PCM-B), and PCM-B in powder form (pPCM-B). The characterization of PCM and soil-PCM mixture was determined by Atterberg limits, Harvard miniature compaction test, differential scanning calorimetry (DSC), scanning electron microscope (SEM) imaging, freezing point depression and PCM evaporation tests. DSC tests confirmed that the selected PCMs have high latent heat. Freezing point depression tests showed that PCM-B and pPCM-B freeze above the freezing point of water in soil, suggesting they would delay the freezing of soil. SEM images showed no change on the surface of soil-PCM mixtures compared to the control specimens, indicating no chemical reaction between soil and PCMs occurred. PCM-B did not evaporate from the surface of soils for a 2-hour period at various environmental conditions. Based on characterization tests, PCM-B was selected as the best-performing PCM, and it was tested for further performance tests such as resilient modulus (M_R), frost heave-thaw settlement tests. PCM-B did not cause an adverse effect on the M_R of GT at different number of freeze-thaw cycles. PCM-B showed a good thermoregulation effect and slowed down the water migration in the frozen region of soil by reducing the permeability of the soils. Furthermore, after 2 F-T cycles, all soils with PCM-B achieved significantly lower heave rate, maximum heave and moisture content than control specimens. The results suggest that PCMs can be highly effective at mitigating freeze-thaw damage in subgrade soil.

This thesis is dedicated to my father, mother, my siblings and my mentors. I am so grateful to all of which for their continuous support in my journey.

ACKNOWLEDGEMENTS

I would like to thank my advisor, Dr. Bora Cetin, for giving me the opportunity to work on my graduate studies and for supporting me with his guidance, wisdom, and motivational efforts. His feedback helped me to improve my technical writing and presentation skills, as well as critical thinking. I also would like to express my appreciation to my committee members, Dr. Kristen Cetin and Michele Lanotte for their precious contribution to my research studies. Their feedback and support helped me to improve the quality of my work.

I would like to acknowledge and thank Iowa Highway Research Board (IHRB) for providing financial resources for this study.

I am also grateful for the support, assistance, and continuous encouragement provided by the staff of Michigan State University - Department of Civil and Environmental Engineering. Special appreciation is also given to individuals who played vital roles throughout my project, including Brian Getzel, the lab manager, and fellow PhD students: Mehdi Bulduk, Oguzhan Saltali, Naqvi Wasif, Fyaz Sadiq, Celso Santos, and Ceren Aydin. Their insightful guidance and physical contributions have been critical to my studies.

Last but not least, I want to express my deepest love to my parents and sisters for their unwavering support and encouragement.

TABLE OF CONTENTS

CHAPTER 1 INTRODUCTION	1
1.1 LITERATURE REVIEW	1
1.2 RESEARCH GOAL AND OBJECTIVES	6
1.3 ORGANIZATION OF THE DISSERTATION	6
CHAPTER 2 CHARACTERIZATION OF SOIL AND PHASE CHANGE MATERIALS	7
2.1 PHYSICAL PROPERTIES OF SOILS	7
2.2 SELECTION OF PHASE CHANGE MATERIALS (PCM)	8
2.3 CHARACTERIZATION OF PHASE CHANGE MATERIALS (PCM)	9
CHAPTER 3 CHARACTERIZATION OF SOIL-PCM MIXTURES	12
3.1 METHODS	12
3.2 RESULTS	18
3.3 SELECTION OF BEST-PERFORMING PCM AND CONCLUSIONS	26
CHAPTER 4 PERFORMANCE TESTS	28
4.1 METHODS	28
4.2 RESULTS	31
CHAPTER 5 CONCLUSIONS AND RECOMMENDATIONS	42
5.1 SUMMARY	42
5.2 CONCLUSIONS	42
5.3 RECOMMENDATIONS	44
REFERENCES	45
APPENDIX: SEM COMPARISON OF CONTROL AND PCM-TREATED SPECIMENS	49

CHAPTER 1 INTRODUCTION

1.1 LITERATURE REVIEW

In cold regions of the world, such as Europe and North America, pavements deteriorate significantly due to freezing and thawing of subgrade soil (Rempel, 2007). In regions experiencing seasonal freezing temperatures, the accumulation of the incremental damage from each freeze and thaw (F-T) cycle results in failure or low performance of roads (Cetin et al., 2019). Such damage to the infrastructure can negatively affect the economy of countries such that the repair or replacement of pavements can cost over 2 billion dollars in the U.S.A. (DiMillio, 1999). If no repair or replacement takes place, the quality of driving experience decreases significantly, and the wear and tear of vehicles becomes easier. Thus, a solution addressing this problem is highly important.

The combined effect of freezing and thawing in soil is described as frost action (Li et al., 2014). Frost action occurs when three factors take place simultaneously: freezing temperatures, frost-susceptible soil, and a water supply (Johnson, 2012). The degree of the frost-susceptibility of any soil is determined by the magnitude of suction and permeability of soil (Carter & Bentley, 2016). There should be enough suction and permeability in soil for frost action to take place. Generally, suction pressure increases with smaller particle size. Therefore, clayey soils would have the highest matric suction. However, they have low permeability to allow for water migration during freezing. On the other hand, coarse-grained materials have high permeability and very low suction due to the large pore size between particles. Silty soils have the characteristics of moderately high suction and medium permeability. Thus, they are commonly referred to as the most frost susceptible soil type (Naqvi et al., 2023). Water supply is also a significant contributor to the frost action. The ice lens growth can only be generated by the migration of water from nearby supplies. This migrated water is responsible for most of the heaving rather than the stationary water (Sadiq et al., 2023).

During the freezing period, freezing temperatures advance into the soil at the freezing front, which is the line where the warmest pore ice exists (Miller, 1972). A special region called the frozen fringe is located between the warmest ice lens and the freezing front (Miller, 1972). Liquid water can exist in the frozen fringe between ice and soil particles due to the adsorption forces and curvature at the soil surface, which leads to a reduction in the free energy of the system (Takagi, 1979). The presence of liquid water creates enough permeability for water migration in the frozen

fringe (Rempel, 2007). The interaction between ice and soil particles causes cryogenic suction to develop in this region, resulting in water migration to the frozen fringe from nearby unfrozen water sources (Rempel, 2007; Thomas et al., 2009). The movement of water from the unfrozen region to the frozen fringe feeds the ice lens and causes it to grow and expand. Eventually, the ice lens becomes big enough to decrease the permeability of the soil and stop water migration to this region. This is followed by a new ice lens formation and frozen fringe positioning at a lower depth. The pressure of the ice lens can be high enough to cause a stress of 334 MPa (Hoekstra, 1969; Tiedje, 2015). The pavement surface will be affected most by heaving since it is in unrestrained condition. Additionally, frost penetration can be non-uniform due to the heterogeneity of soil medium. This results in uneven ice lens pressure on the surface that leads to differential frost heaving and subsequent damage to pavements (Sheng et al., 2013).

Frost heave is followed by a thawing weakening period that causes a reduction in the bearing capacity of soil (Naqvi et al., 2023). Thaw weakening occurs in the spring when accumulated ice during frost action starts melting and creates excess moisture and pore water pressure above the frozen soil, leading to a decrease in the stiffness of subgrade soil and pavement damage under high loadings (Doré, 2004). Frost heaving can vary from year to year. Changes in moisture content, groundwater table, temperatures, and heterogeneity of soil are all factors affecting the degree of frost heave (Isotalo, 1995).

Mitigation efforts have been made for the frost action. Seasonal load restrictions (SLR) are common methods that restrict the weight of vehicles during certain times of the year when spring thaw weakening renders pavements susceptible to damage from high vehicle loads. However, SLR causes a burden on the local economies due to the rerouting of trucks, longer storage time, increased number of trips, and changes in traffic flow (Levinson et al., 2005). Kestler et al. (2007) offered low-cost techniques for implementing SLR at only critical times. Increasing the thickness of granular layers is another common solution to insulate subgrade to protect against frost penetration (Dore, 2020), but it increases the cost and is not preferred in low-volume roads. Henry & Holtz (2001) used geocomposites made from geotextile and geonet as a capillary barrier. However successful results from this geosynthetic depend on the saturation of the soil and water table levels. Oflaherty & Andrews (1968) used three types of lime and cement stabilizers; however, their performance is based on minerals in soil and clay content, thus not offering a comprehensive solution. The chemical stabilizers also exhibit that they are losing their efficiency and performance

over time (Mahedi et al., 2019). These efforts show that more effective solutions are needed. Therefore, this study investigates and evaluates the use of Phase Change Materials (PCM) to mitigate the harmful effect of frost action in subgrade soils.

Phase change materials (PCMS) are widely used as thermal regulators in many applications such as in buildings, transportation, medical fields, and solar water heating systems (Anupam et al., 2020). When the temperature drops below the freezing temperature of PCM, PCM releases a high amount of heat and warms up the surrounding space, causing a damping effect on the reduction of temperature. Similarly, when the temperature goes up above the melting temperature of PCM, PCM absorbs a high amount of heat from the environment and slows down the increase in temperature. This way, PCMs can reduce the severity of temperature fluctuations around their freezing/melting point. In this study, PCMs are expected to reduce the detrimental effects of freeze-thaw (F-T) cycles in soil by thermoregulation mechanism. Studies in the past show that PCMs can minimize temperature fluctuations. Castell et al. (2010) showed that PCM incorporation in construction materials causes a reduction in temperature fluctuations and energy consumption by 15% compared to the insulating material. Chen et al. (2012) showed that PCM in asphalt can slow down the heating and cooling rate of asphalt. Ma et al. (2011) also reported that PCM in asphalt reduces the maximum temperature when heated and increases the minimum temperature during cooling. Similarly, in the study of Yeon & Kim (2018), PCM in concrete pavement reduced the temperature fluctuations near its freezing/melting point. In a study conducted by Hawe et al. (1989), PCM-incorporated concrete had better freeze-thaw resistance compared to the control specimen. Kravchenko et al. (2020) and Mahedi et al. (2019) showed that PCM in soil achieves higher temperatures during freezing due to the high latent heat.

In a PCM-soil mixture, the freezing and melting of soil will be delayed by the use of PCM latent heat. The temperature fluctuations around 0 °C in soil will be less severe, and the number of freeze-thaw cycles will be fewer in any given year. Consequently, the pavement lifespan will be extended. The selection of PCM is critical for any PCM application. An ideal PCM must have high latent heat, high thermal conductivity, and high specific heat for better thermoregulation. It should be stable after many F-T cycles and have minimum volume change. Minimum or no supercooling is desired, as supercooling would cause PCM to miss the target freezing point. It should also have good environmental properties, including being non-flammable, non-corrosive, and non-toxic (Anupam et al., 2020). Si et al. (2015) suggested a temperature range between -5 °C to 5 °C for

PCM melting point in low-temperature thermoregulation of pavement, which can be taken as a reference for soil application.

PCMs can be divided into three types: organic, inorganic, and eutectic mixtures (Cabeza et al., 2011). Organic PCMs are the most popular choice because they are readily available, not expensive, and easy to handle (Fleischer, 2015). Organic PCMs have two main groups: paraffin and non-paraffin PCMs. Commercial-grade paraffins are inexpensive, safe, reliable, and non-corrosive (Sharma et al., 2009). Non-paraffins are divided into fatty acids, alcohols, esters, and glycols categories (Anupam et al., 2020). Inorganic PCMs can be divided into two categories: salt hydrate and metallic PCMs. Salt hydrates are composed of dissolved inorganic salts in water. Metallic PCMs consist of metals. They tend to have a very high freezing/melting temperature, which makes them suitable only for high-temperature applications (Kalnaes & Petter Jelle, 2015). Eutectic mixtures are made of two or more PCMs. Eutectic PCM properties can be altered by adjusting the weight of components (Su et al., 2015). This way, the PCM mixture would provide flexibility in targeting different temperature ranges. Further information on each type is shown in Table 1. (Tyagi et al., 2022; Zhou et al., 2011).

There are many techniques to incorporate PCM into materials, such as microencapsulation, nanoencapsulation, shape stabilization, and embedded tubes (De Matteis et al., 2019; Farnam et al., 2017; Huang et al., 2018; Mahedi et al., 2019). All the encapsulation techniques aim to prevent the leakage of PCMs and the reduction in the mechanical performance resulting from the interaction between PCM and the surrounding material. Microencapsulation is the encapsulation of PCM with a shell size between 1 μm and 10^{-3} mm. (Anupam et al., 2020). The disadvantage of microencapsulation is that they burst when mixing or under loading, and cause a reduction in the mechanical strength. They also increase the cost significantly. Macroencapsulation is the encapsulation of PCM with a shell size of more than 1mm. (Anupam et al., 2020). It has a relatively low cost and overcomes the mechanical problems that microencapsulation has (Castell et al., 2010). The drawback of macroencapsulation is that it has a lower surface area which causes poor thermal conductivity. Nanoencapsulation is the encapsulation of PCM with a shell size of less than 10^{-6} mm. (Anupam et al., 2020). De Matteis et al. (2019) obtained better overall thermal performance for nanoencapsulation compared to microencapsulation due to the increased specific surface of silica nanoparticles, resulting in an increased heat transfer rate. According to Wang et

al. (2015), reducing the particle size of encapsulated PCMs enhances their mechanical stability and mobility. However, they are not readily available as they are rarely fabricated and costly.

Table 1. 1 The advantages and disadvantages of organic, inorganic, and eutectic PCMs (Tyagi et al., 2022; Zhou et al., 2011)

Classification	Advantage	Disadvantage
Organic PCMs	Availability in a large temperature range High heat of fusion No supercooling Chemically stable and recyclable Good compatibility with other materials	Low thermal conductivity Low latent heat Relatively large volume change during phase change Flammability
Inorganic PCMs	High heat of fusion High thermal conductivity Low volume change Availability in low cost Sharp melting point	Supercooling Corrosion (metallic PCMs) Incongruent melting Non compatibility with metals Chemically and thermally unstable
Eutectics	High volumetric thermal storage density Little super cooling Good thermal/chemical stability Sharp melting point	High Cost Low heat transfer Leakage during phase change Lack of data regarding thermo-physical properties

In the shape stabilization technique, PCM is absorbed by a porous carrier. For example, vacuum impregnation is one of the ways to achieve that. PCMs are held inside the porous space by the capillary force and surface tension. (Anupam et al., 2020). A drawback of this technique is that the amount of PCM absorption can be limited. PCMs in small tubes can be another way of incorporating PCM into the soil. Farnam et al. (2016) compared the performance of shape stabilization (lightweight aggregate filling) to PCM embedded tubes and found that embedded

tubes showed superior performance. In this study, organic liquid, inorganic liquid, and PCM in powder form were evaluated for incorporation in soil.

1.1 RESEARCH GOAL AND OBJECTIVES

Two primary objectives are established in this study:

- **Characterization of soil-PCM mixtures and Selection of Best-Performing PCM**

Three types of PCM were incorporated into two soil types and the impact of PCM on soils was analyzed by the results obtained from Atterberg limits, scanning electron microscope (SEM) images, differential scanning calorimetry (DSC), Harvard miniature compaction test, PCM evaporation and freezing point depression tests. One of the PCMs was selected as the best-performing PCM to mitigate the damage of frost action.

- **Performance Testing of the Selected PCM**

The effect of the best-performing PCM on the soil's frost heaving, thaw settlement, temperature profile, moisture profile, and stiffness was tested by frost-heave and thaw settlement test and resilient modulus (M_r). Specimens were subjected to freeze-thaw (F-T) cycles during these tests, measuring the freeze-thaw resistance impact of PCMs in soils.

1.3 ORGANIZATION OF THE DISSERTATION

This dissertation consists of five chapters. Chapter 1 provides a literature review on the frost action problem, the history of solutions, and phase change materials (PCM). Chapter 2 gives information about soils and PCMs used in this study. Chapter 3 explores the characterization of soil-PCM mixtures to compare three PCMs and suggests one PCM as superior. Chapter 4 conducts subgrade performance tests on the superior PCM earlier found in Chapter 3. Chapter 5 summarizes this study and provides conclusions and recommendations for future studies. The conclusions for Chapter 4 are merged with the overall conclusions in Chapter 5.

CHAPTER 2 CHARACTERIZATION OF SOIL AND PHASE CHANGE MATERIALS

Two distinct subgrade materials, named Glacial Till (GT) and Sandy Soil (SS), were obtained from Loess Hills Missouri Alluvial Plains and Pottawattamie County in Iowa, respectively. Three commercial PCMs (PCM-A, PCM-B, and pPCM-B) were selected for characterization tests based on the literature review. Chapter 2.1 and Chapter 2.2 detail the soil and PCM properties.

2.1 PHYSICAL PROPERTIES OF SOILS

The grain size distributions of the soils were determined in accordance with ASTM C136/C136M. Fine and coarse aggregates were separated following ASTM C117. Figure 2.1 shows the grain size distributions of the soils. GT consists of 64% silt, 29% clay, and 7% sand grains, while SS is composed of 9% silt, 3% clay, and 88% sand grains.

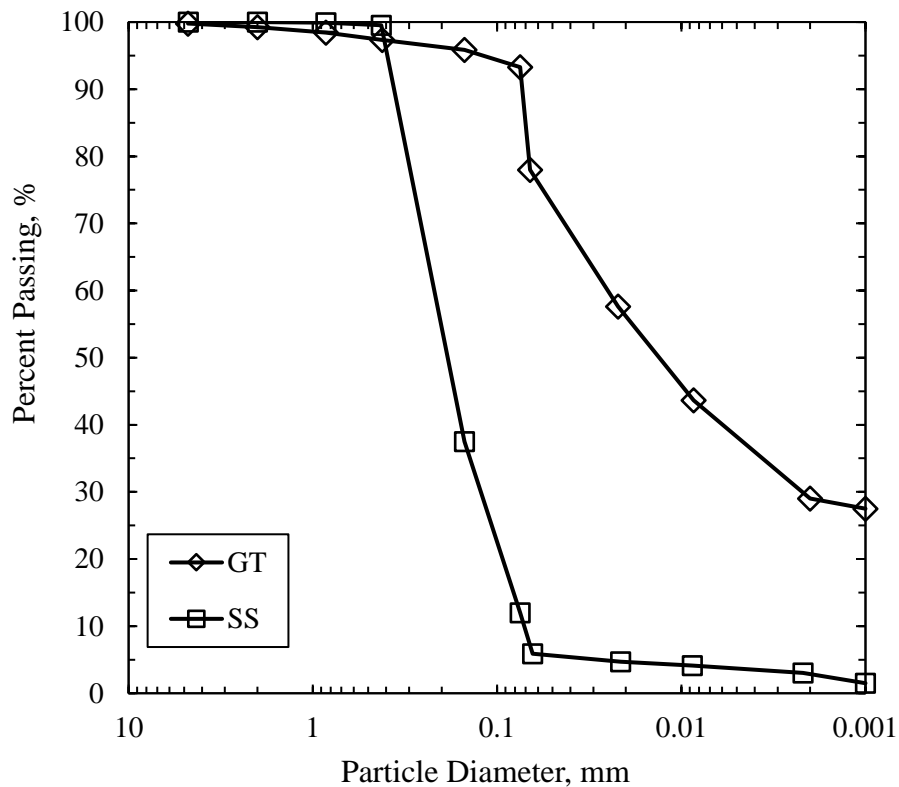


Figure 2. 1 Grain size distribution of Glacial Till (GT) and Sandy Soil (SS)

Liquid limit (LL) and plasticity index (PI) of the soils were determined following ASTM D4318. Optimum moisture content (OMC) and maximum dry unit weight (MDU) were determined

in accordance with ASTM D698-12. The physical properties of soils are summarized in Table 2.1. Based on the index properties, GT is classified as a lean clay and A-7-6 according to the Unified Soil Classification System (USCS) (ASTM D2487) and AASHTO classification (AASHTO M 145), respectively. SS is classified as a poorly graded sand with silt and A-2-4 according to USCS and AASHTO, respectively. SS soil is a non-plastic soil. Based on the index properties it was determined that GT is a frost susceptible soil for which PCM application can be useful.

Table 2. 1 Grain size distribution of Glacial Till and Sandy Soil

Properties	Glacial Till (GT)	Sandy Soil (SS)
Gravel (%)	0	0
Sand (%)	7	88
Silt Content (%)	64	9
Clay Content (%)	29	3
LL (%)	48	NP
PI (%)	23	-
MDU (%)	16.4	17.1
OMC (%)	20	14.5
USCS	CL	SP-SM
AASHTO Classification	A-7-6	A-2-4

LL = Liquid Limit; PI = Plasticity Index; MDU = Maximum Dry Unit Weight; OMC = Optimum Moisture Content; USCS = Unified Soil Classification System; AASHTO = American Association of State Highway and Transportation Officials; NP = non-plastic

2.2 SELECTION OF PHASE CHANGE MATERIALS (PCM)

The freezing/melting range is one of the most important factors when selecting the right PCM. The freezing/melting range should match with the target temperature range, at which the latent heat is needed to slow down temperature change. In the case of mitigating damage from frost action, PCMs should undergo a phase change at a temperature range slightly above the freezing point of water in the soil, which is around -1 to 0 °C, depending on the salt content of the soil medium. 0 to 5 °C can be considered a good range for PCM in soil application. When PCM freezes in this range, it will heat the environment and the soil will take a longer time to reach 0 °C. When the temperature warms up above 5 °C, PCM will melt, and its latent heat can be used again when freezing temperatures are in contact with soil.

Three types of commercial PCMs were procured based on the PCM selection criteria described earlier. PCMs were named PCM-A, PCM-B, and pPCM-B, and they are shown in Figure 2.2. Table 2.2 also presents the physical properties of PCMs. Freezing/melting points represent the values obtained from the respective companies. PCM-A is a viscous inorganic salt hydrate with water as the solvent. It expands by about 9% when frozen. PCM-B is a transparent organic liquid that shrinks about 4% when frozen. pPCM-B consists of approximately 50% PCM-B and 50% absorbent material by weight. Having 50% absorbent material with no latent heat makes pPCM-B less efficient in latent heat per unit mass compared to PCM-B.



Figure 2. 2 PCMs used in the study (from left to right: PCM-A, PCM-B, and pPCM-B)

Table 2. 2 Physical Properties of Phase Change Materials

Property	PCM-A	PCM-B	pPCM-B
Latent Heat (J/g)	197.4	106.4	67.6
Specific Gravity	1.01	0.76	NA
Freezing & Melting Point (°C)	0.5	2.2	2.2
Kinematic Viscosity (mm/s) at 21 °C	4.6	2.4	NA
PCM Phase	Liquid	Liquid	Powder
PCM Type	Inorganic	Organic	Organic
Volume Change During Freezing	+9 %	-4%	NA

NA = not available

2.3 CHARACTERIZATION OF PHASE CHANGE MATERIALS (PCM)

The phase change temperature range and latent heat of the PCMs were measured by differential scanning calorimetry (DSC) test. TA Instruments Model Q2000 was used as the testing equipment. During the experiment, samples weighing 10-30 mg were subjected to an initial temperature of 20 °C, followed by cooling down to -15 °C and then heated up to 20 °C at the end. The rate of cooling and heating was kept at 1.0 °C/min throughout the experiment.

Figure 2.3 shows the DSC curve for each PCM. The machine was unable to detect heat flow during the freezing of PCM-A, indicating that PCM-A requires a longer time to freeze due to supercooling. Despite lowering the rate of cooling for PCM-A, no heat flow was detected a second time. This may be attributed to the machine's incapability to detect heat flow at a very low heating/cooling rate.

DSC results show that PCM-A melts between $-3.3\text{ }^{\circ}\text{C}$ and $5.5\text{ }^{\circ}\text{C}$, with a peak melting temperature of $1.4\text{ }^{\circ}\text{C}$. The latent heat energy for melting is 197.4 J/g , which is the highest among all three PCMs. The water portion of PCM-A could be the reason for the high latent heat, as water has a high latent heat capacity (334 J/g). PCM-B has a peak freezing temperature of $-0.1\text{ }^{\circ}\text{C}$ and a peak melting temperature of $2.0\text{ }^{\circ}\text{C}$. The latent heat energy of PCM-B for freezing and melting is 103.8 J/g and 106.4 J/g , respectively. The peak freezing temperature of pPCM-B is $-2.7\text{ }^{\circ}\text{C}$, while the peak melting temperature is $0.7\text{ }^{\circ}\text{C}$. The latent heat energy for freezing and melting is 68.9 J/g and 67.6 J/g , respectively. The lower latent heat of pPCM-B could be attributed to the presence of an absorbent material. The absorbent material takes up about 50% of the weight and produces no latent heat. Consequently, the overall pPCM-B compound has a low latent heat.

PCMs can exhibit a different phase change temperature range in a soil-PCM mixture. Soil-PCM interaction and the amount of PCM can affect the phase change temperature. Therefore, the freezing point depression test would be a better indicator regarding the phase change temperature range of PCMs.

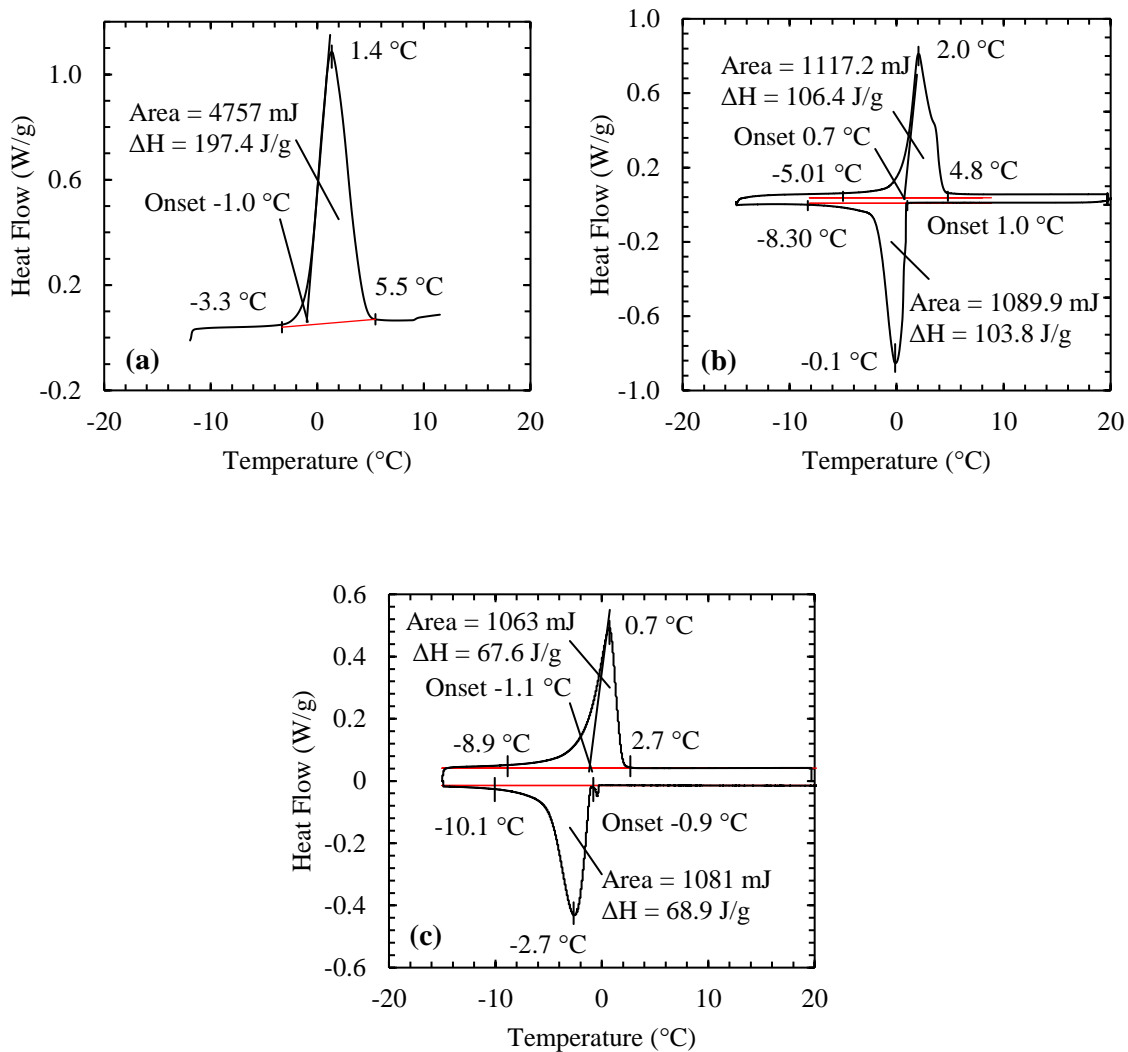


Figure 2. 3 DSC curve for (a) PCM-A, (b) PCM-B, and (c) pPCM-B

CHAPTER 3 CHARACTERIZATION OF SOIL-PCM MIXTURES

3.1 METHODS

The characterization of soil-PCM mixtures is achieved by the test results of Atterberg limits, Harvard miniature compaction test, scanning electron microscope (SEM) images, PCM evaporation, and freezing point depression tests. To investigate the effect of PCM at different concentrations, PCM-A and PCM-B were mixed into soils at concentrations of 5%, 10%, and 15% by weight of the dry soil. pPCM-B is mixed at 10% and 20% by weight. Since 50% of pPCM-B by weight is composed of the absorbent material, 10% and 20% of pPCM-B correspond to 5% and 10% PCM-B concentration. These contents were used for most of the characterization experiments. All results are compared with control specimens and each other. Table 3.1.1 presents the notation used to display the results of soil-PCM mixtures and the control specimens.

Table 3. 1. 1 Test matrix and notations of soil-PCM Mixtures and control specimens

Glacial Till	GT	GT-A5	GT-A10	GT-A15	GT-B5	GT-B10	GT-B15	GT-pB10	GT-pB20
PCM (%)	0	5	10	15	5	10	15	10	20

Sandy Soil	SS	SS-A5	SS-A10	SS-A15	SS-B5	SS-B10	SS-B15	SS-pB10	SS-pB20
PCM (%)	0	5	10	15	5	10	15	10	20

GT = Glacial Till; SS = Sandy Soil; A = PCM-A; B = PCM-B; pB = pPCM-B

The letters before the hyphen indicate the type of soil. Glacial Till and Sandy Soil are abbreviated as GT and SS. GT and SS, without any additional letter, indicate control specimens with no PCM addition. After the hyphen; A, B, and pB refer to PCM-A, PCM-B, and pPCM-B, respectively. The number next to PCM letters indicates the percentage of PCM by weight in the mixture. 5%, 10%, and 15% were used for PCM-A and PCM-B, while 10% and 20% concentrations were used for pPCM-B. Since PCM-B has approximately 50% PCM by weight, 10% and 20% correspond to 5% and 10% of PCM.

3.1.1 Atterberg Limits:

Atterberg limits are fundamental properties of any soil. Therefore, the impact of PCMs on them needs to be assessed. The liquid limit (LL), plastic limit (PL), and plasticity index (PI) of the soil-PCM mixtures and the control specimens were determined following ASTM D4318. Oven-dried soils were mixed by hand with PCM-A and PCM-B at 5%, 10%, and 15% by weight and with pPCM-B at 10% and 20% by weight. All tests were conducted shortly after sample

preparation. Triplicate samples weighing 15-20g were obtained to determine the PL. The Atterberg limits were only obtained for GT-PCM mixtures since SS is a non-plastic soil.

As shown in Figure 3.1.1, PCM-B leaks out from the soil when water is added to the soil-PCM mixture. The leakage is more significant at a higher water or PCM-B content, leading to a lower LL value than the actual measurement. Table 3.1.2 illustrates an example of how the actual moisture content will be higher in the case of leaking PCM-B. Only the total liquid content could be measured by evaporating all the liquid at high temperatures. The initial PCM content was known since PCM addition was measured before mixing. Thus, under the assumption of no leakage, water content can be measured by subtracting the initial PCM content from the total liquid content. However, in the case of leakage, the initial PCM content will be lowered during mixing or compacting, and the water content will have to be higher to achieve the same liquid content.



Figure 3. 1. 1 Leakage of PCM-B during Liquid Limit Test

The results are obtained under the assumption of no leakage of PCM-B since the amount of leaking PCM could not be measured. Consequently, the actual water content of some measurements should be higher than the measured values. No leakage was observed during the PL testing, which is likely due to the low water content. Thus, the leakage only influenced the results of the liquid limit and the PI.

Table 3. 1. 2 The Effect of Leakage on Results

Assumption	Water (%)	PCM-B (%)	Evaporated Liquid Content (%)
No leakage	15	15	30
PCM-B leaking	>15	<15	30

3.1.2 Harvard Miniature Compaction Test:

The effect of PCM on soil compaction behavior is tested by following ASTM SPT479. Harvard miniature compaction test serves as an alternative to the Proctor Compaction test and involves smaller sample amounts. The specimen was compacted into a cylindrical mold with an internal diameter of 33.3 mm and a height of 71.6 mm. Five layers were created, with ten tamps applied to each layer.

The same test matrix as in Atterberg Limits was utilized. PCM-A and PCM-B were mixed at 5%, 10%, and 15%, while pPCM-B was mixed at 10% and 20% by weight. Results were then compared with each other and with control specimens. Similar to the Atterberg Limits testing, leakage of PCM-B was observed during the test. This occurred at a lower water or PCM-B content because the force of compaction triggered PCM-B leakage more easily.

3.1.3 Scanning Electron Microscope (SEM) Imaging:

A microscopic view of soil-PCM mixtures and control specimens was obtained using scanning electron microscope (SEM) images. The literature shows that a chemical reaction between soil and certain chemicals, such as stabilizing agents, can be detected in SEM images (Coban & Cetin, 2022). Therefore, SEM images can be valuable data to determine whether PCMs react with the soil. To utilize the thermoregulatory properties of PCM, no chemical reaction should occur between PCM and the soil. If such a reaction occurs, PCMs will turn into a different chemical, resulting in the loss of their high latent heat properties.

Images were captured at magnification factors of 500, 1000, 1500, and 5000x. A low coating at the surface and 10kV energy were applied to the specimens. As part of obtaining images from SEM, a vacuum was applied to the specimens before capturing images. This process causes liquids or loose materials to be vacuumed out, hence they would not be visible in the images. The soil-PCM mixtures contained only 10% of each PCM type. A 12-day stabilization period was applied to account for the possibility of a slow rate of reaction between PCMs and soil.

3.1.4 PCM Evaporation:

Liquid PCMs can evaporate during the time between the mixing of soil and compaction stages in the field. Therefore, the evaporation behavior of PCMs needed to be studied through the PCM evaporation test. These tests were conducted at temperatures of 20 °C, 35 °C, and 50 °C at humidity levels of 25%, 50%, and 75%. Test specimens consisted of 250 grams of oven-dried soil. PCM-A and PCM-B were mixed with the soil at 5%, 10%, and 15% by weight. Given that surface area is a critical factor in liquid evaporation, dimensions were kept constant at 89 mm x 190 mm. The specimens were placed in an environmental chamber that was adjustable for both the target temperature and humidity levels. The humidity chamber is shown in Figure 3.1.2. Generally, there is a two-hour delay between mixing and soil compaction in the field. Thus, the two-hour evaporation rate of soil-PCM mixtures was measured. The initial total mass at time $t = 0$ and the final total mass at $t = 2$ hours were recorded. The difference between them was divided by the mass of the initial PCM amount added to the soil, yielding the percentage of PCM loss. Finally, the percentage of the remaining PCM was obtained by subtracting the percentage of PCM loss from 100.

$$\% \text{ of PCM Loss} = \frac{\text{Final Total Mass}(t = 2 \text{ hours}) - \text{Initial Total Mass}(t = 0)}{\text{Mass of PCM mixed with soil}}$$

$$\% \text{ of Initial PCM} = 100 - \% \text{ of PCM Loss}$$



Figure 3. 1. 2 PCM Evaporation Test Setup

3.1.5 Freezing Point Depression Test:

The freezing curves of soil-PCM mixtures, soil-water mixtures, and soils were determined following ASTM D5918. During the temperature decrease, soils have a typical declining cooling curve. The cooling curve increases slightly during the phase change of water. The latent heat released by water is absorbed by the soil, resulting in a small temperature increase as shown in Figure 3.1.3. The latent heat of PCM can be detected in a similar fashion. However, if the latent heat of PCM is not high enough, instead of a significant jump in temperature, a change in the slope of the declining curve (decreasing angle with horizontal) can be observed. This would also suggest the freezing of PCM in the specimen.

The equilibrium temperatures outlined by ASTM D5918 were changed to 5 °C and -5 °C to observe the potential freezing of PCMs within this temperature range. Control specimens (soil alone), which had no water or PCM, soil with water at optimum moisture content (14.5% for SS and 20% for GT), and soils containing PCM-A and PCM-B at 5%, 10%, and 15%, were placed in

a plastic tube at a height of 20.3 mm. Water mixed with ethylene-glycol is capable of reaching lower temperatures than 0 °C without freezing of water in the solution. A cold bath containing a mixture of 50% ethylene-glycol and 50% water by volume was used to cool down the specimens. The sample tube was inserted into the mixture in such a way that the top of the specimens stayed 10 mm below the liquid surface. The real-time temperature of the specimen was obtained.

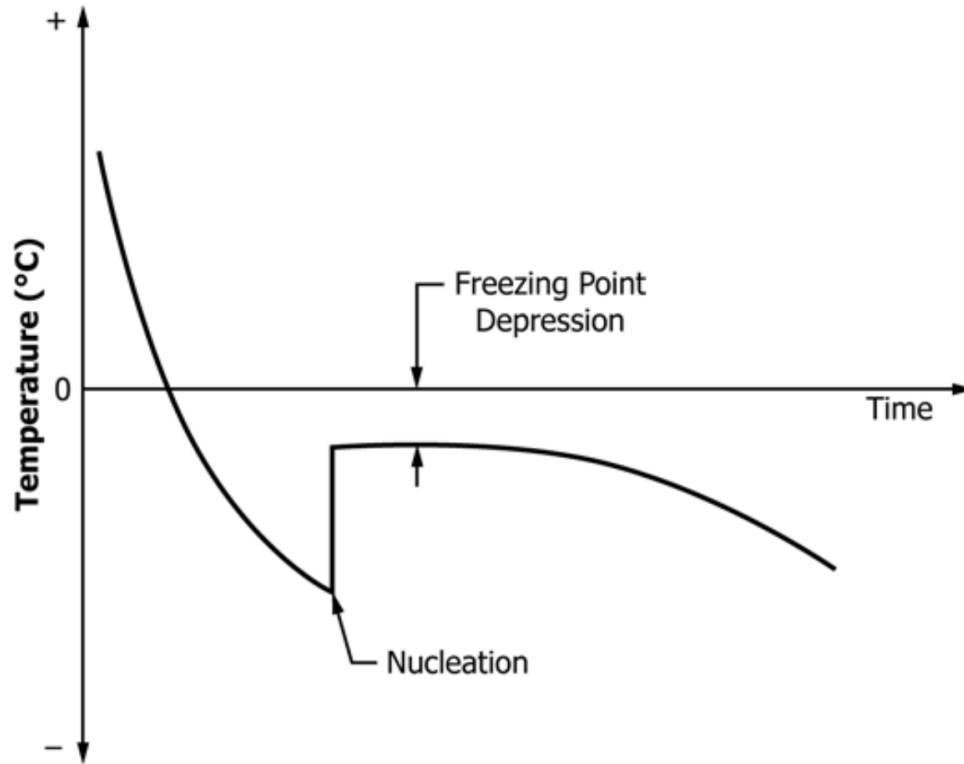


Figure 3. 1. 3 Obtaining Freezing Point Depression from Cooling Curve (ASTM D5918)

The results provide better insight into the freezing range of PCMs than differential scanning calorimetry (DSC) results, as the freezing range can be affected by PCM-soil interaction and the PCM amount. Additionally, soil-PCM and soil-water mixture data allow for direct PCM and water comparison in terms of latent heat and melting temperature.

3.2 RESULTS

3.2.1 Atterberg Limits:

Figure 3.2.1 displays the liquid limit (LL), plastic limit (PL), and plasticity index (PI) values of soils with additions of PCM at 5%, 10%, and 15% by weight. LL and PL values decrease with increasing PCM-A content. When the addition of PCM-A is 10%, LL reduces from 48% to 38% in Figure 3.2.1a. Similarly, when PCM-A was 16%, LL decreased by about 16%. The decrease in LL is approximately equal to the addition of PCM-A content. The same effect is also present in PL values in Figure 3.2.1b. The total liquid content (PCM-A + Water) is roughly equal to the LL and PL values of the control specimen. Since the change in LL and PL values are approximately the same, PI (which equals the difference between LL and PL) values remain constant in the range of 21% to 24%. The results suggest that PCM-A behaves like water in terms of changing Atterberg limits. Because the changes in LL and PL are equal to the change in PCM content. The water-like behavior could be attributed to the fact that PCM-A contains water as a solvent.

Increased PCM-B content raises LL and PI by about 10% and 15%, respectively, while lowering PL values by about 5% to 10%. It should be noted that at higher water or PCM-B contents, the leakage of PCM-B was observed. As explained in the methods section, LL values are higher than the actual value due to PCM-B leakage. Thus, in both leakage or no leakage assumption, PCM-B increased LL as shown in Figure 3.2.1a. Mahedi et al. (2019) also observed a similar increase in LL with an organic PCM. Water facilitates the sliding of soil particles on top of each other. LL is reached when the ease of sliding reaches a certain degree (closure of the groove in 25 blows). In a soil-PCM mixture, PCM-B remains between soil and water, preventing some of the water from facilitating the movement. Hence, a higher moisture content is needed to achieve the same required ease of movement for soil particles (closure of the groove in 25 blows). The PL decreases with an increase in PCM-B content. This change could be attributed to the contribution of PCM-B in keeping soil particles together via cohesion and adhesion. As a result of the increase in LL and the decrease in PL, PI increases with the addition of PCM-B. Figure 3.2.1 shows that all Atterberg limits increase dramatically with pPCM-B addition. The absorbent material in pPCM-B absorbs some water, leading to increased values in all three tests.

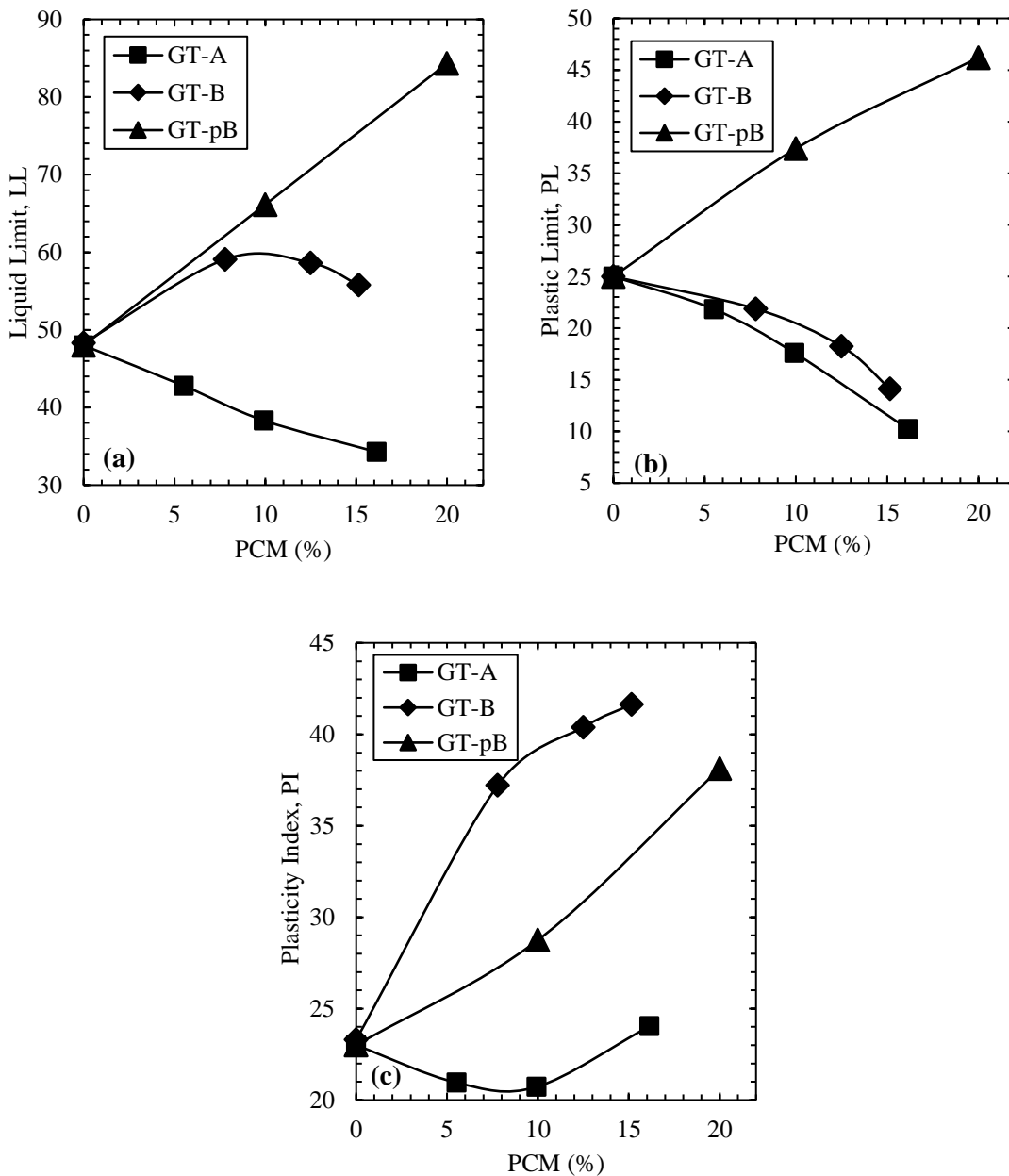


Figure 3. 2. 1 PCM effect on (a) Liquid Limit (LL), (b) Plastic Limit (PL) , and (c) Plasticity Index (PI)

GT = Glacial Till; SS = Sandy Soil; A = PCM-A; B = PCM-B; pB = pPCM-B

3.2.2 Harvard Miniature Compaction Test:

Figure 3.2.2 displays the compaction curve for each PCM type in GT soil. PCM-A decreases the optimum moisture content while keeping the maximum dry unit weight at the same value in GT, as shown in Figure 3.2.2a. The decrease in moisture content is roughly equal to the

addition of PCM. Therefore, the behavior of PCM-A is very similar to water, as was the case for Atterberg limits. PCM-A has a specific gravity of 1.00, the same as water, which accounts for the same maximum dry unit weight. In addition, since PCM-A is salt-hydrate and contains water, it provides the same lubricating effect as water; thus, the same dry unit values were obtained.

PCM-B decreases the maximum dry unit weight in GT as shown in Figure 3.2.2b. The lower unit weight of PCM-B, which is 7.45 kN/m^3 compared to 9.81 kN/m^3 of water, causes the reduction in the maximum dry unit weight values, as PCM-B takes up more space and allows less compaction for soil particles. Mahedi et al. (2019) obtained a similar reduction in dry unit weight with an organic PCM having a lower specific gravity than water. The optimum moisture content decreases slightly with increased PCM-B. The lower specific gravity of PCM-B and increased total liquid content may be the reasons for lower optimum moisture content. The soil reaches the optimum moisture content at a lower moisture content due to PCM-B filling up voids and replacing solid particles. Additionally, due to the leakage of PCM-B, it should be kept in mind that the moisture content values of GT-B10 and GT-B15 could be higher than the true values since the leakage was observed at those PCM-B concentrations.

The impact of pPCM-B on the compaction characteristics of GT is shown in Figure 3.2.2c. pPCM-B decreases the maximum unit weight in GT, which can be attributed to the very low density of pPCM-B. The optimum moisture content increases with pPCM-B addition. This is due to the absorbent material in the pPCM-B compound, which absorbed some moisture in the experiment. The observation also aligns with the increase in the Atterberg limits and suggests that the absorbent material in pPCM-B absorbs some portion of water.

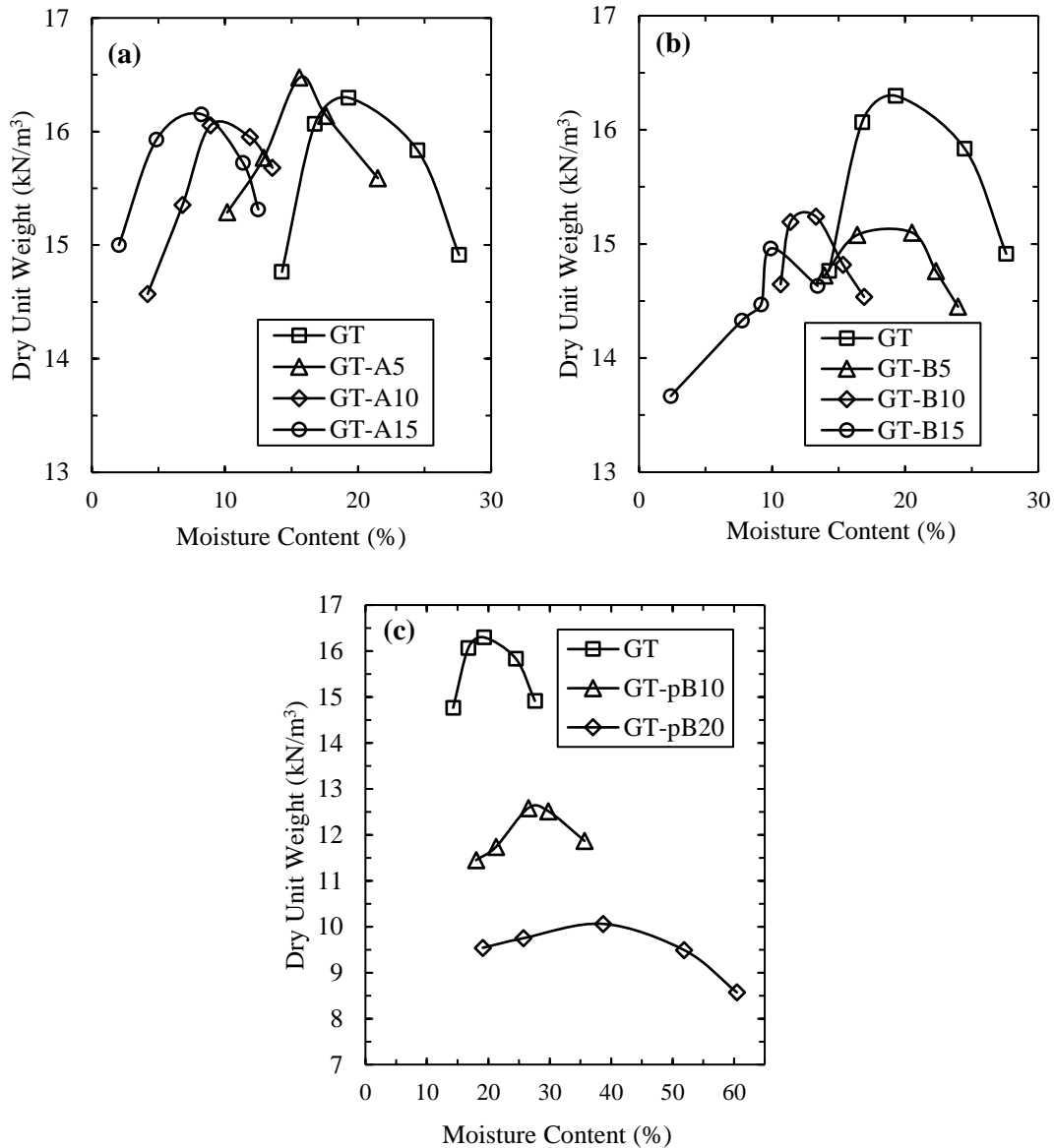


Figure 3. 2. 2 Compaction Curves for GT (a) PCM-A, (b) PCM-B, and (c) pPCM-B

Figure 3.2.2 illustrates the compaction curve for each PCM type in SS soil. Figure 3.2.3a shows that the addition of PCM-A decreases the optimum moisture content, which was also the case for GT. However, it increases the dry unit weight of the soil, as opposed to the reduction of the maximum dry unit weight observed in GT. The high viscosity of PCM-A might provide a better lubricating effect, especially on sandy particles, since sandy grains can exhibit significant interlocking due to their larger particle size. The viscosity of PCM-A helps overcome some of the interlockings among sand grains. A similar effect doesn't occur in fine-grained GT because interlockings are weaker, and water is sufficient to overcome them.

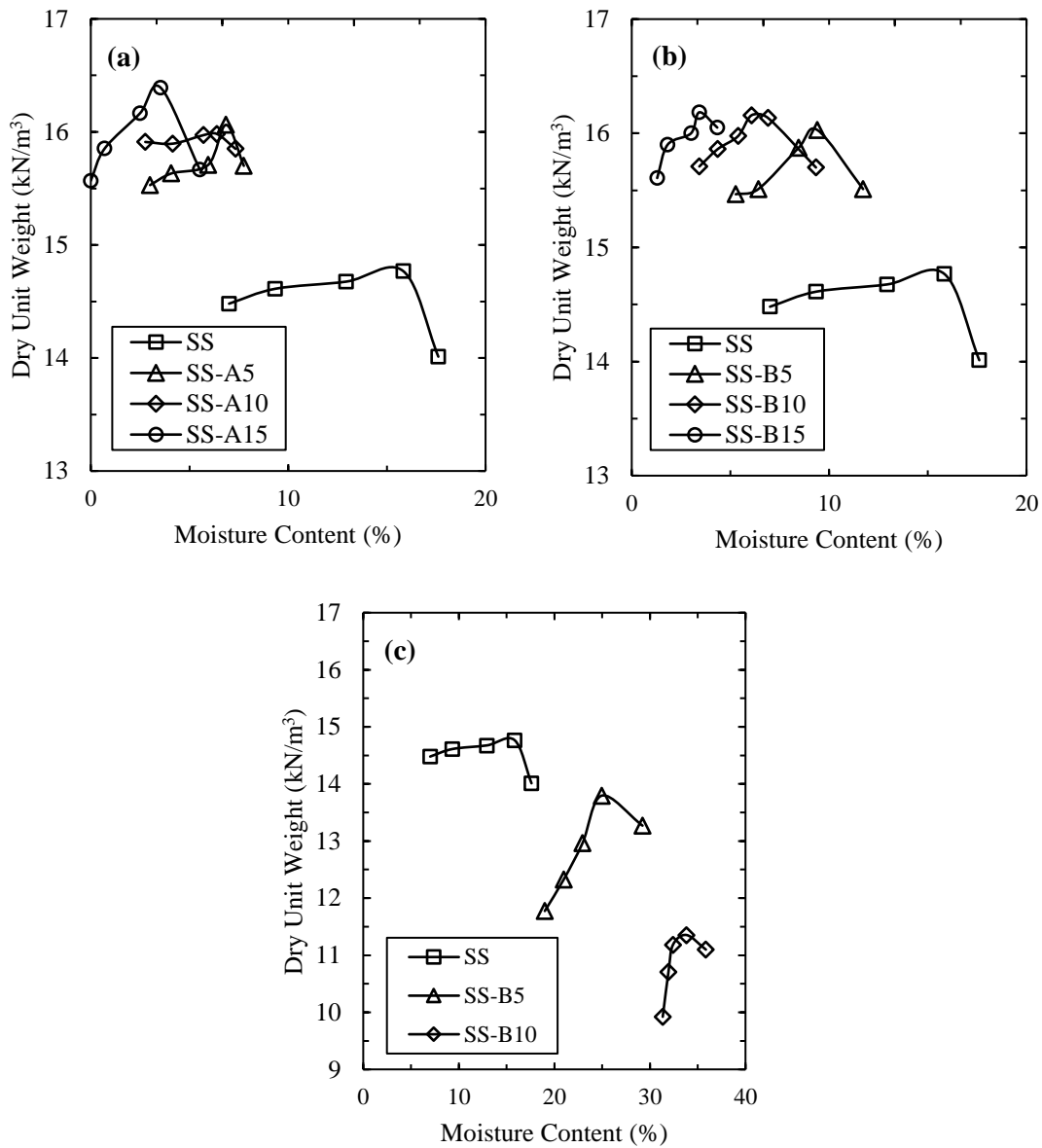


Figure 3. 2. 3 Compaction Curves for SS with (a) PCM-A, (b) PCM-B, and (c) pPCM-B

PCM-B increases the maximum dry unit weight in SS in Figure 3.2.3b, similar to PCM-A. PCM-B also has a higher viscosity than water thus it displays a better lubricating effect than water. However, it can only increase the unit weight of SS, not GT. Because sand grains have stronger interlockings than fine-grained GT. The conclusion was that a higher viscosity of liquid leads to better compaction for coarse-grained materials like sand.

pPCM-B decreases the maximum dry unit weight dramatically, as was the case for GT. The low density of pPCM-B takes up too much space in the mixture. The powders in the

pPCM-B compound also interlock with each other, causing a significant reduction in dry unit weight at all moisture contents. On the other hand, the absorbent material in pPCM-B contributes to the increase in the optimum moisture content by absorbing some of the water content. In conclusion, the dramatic decrease in the dry unit weight makes pPCM-B a much less favorable choice.

3.2.3 Scanning Electron Microscope (SEM) Images:

SEM image comparisons between GT and GT with three types of PCM at different magnification values are shown in Figures A.1, A.2, and A.3 in Appendix. Soil conglomeration can be seen in GT-A10 images due to the adhesion between PCM-A and the soil. The high viscosity of PCM-A caused that effect. Other than that, the surfaces of the soil remained unchanged. No chemical bonding or reaction was observed in any of the images, suggesting that no chemical reactions took place. Figures A.4, A.5, and A.6 in Appendix present SEM image comparisons between SS and SS with three types of PCM at different magnification values. Similar to GT, the SEM images of SS reveal no significant changes between the control specimen and soil-PCM mixtures, also suggesting that no chemical reactions occurred between PCMs and the soil. Having no chemical reaction is a desired outcome. If there was a reaction, PCMs would have transformed into different chemicals and lost their high latent heat.

3.2.4 PCM Evaporation:

The evaporation of PCMs is shown in Table 3.2.1. The values represent the percentage of PCM remaining after 2 hours at specific temperature and humidity conditions. As shown in the results of A5, A10, and A15 in both soils, PCM-A exhibits significant evaporation in most of the environmental conditions, suggesting that a higher percentage should be initially mixed to achieve the target PCM-A ratio. The evaporation of PCM-A is attributed to the water portion inside PCM-A. The evaporation is higher in SS than in GT for PCM-A. GT contains silt and clay particles with charged surfaces. These charged surfaces can attract PCM-A more strongly than sand particles, resulting in higher adhesion forces and less evaporation. Evaporation is much higher at high temperatures and low humidity levels. High temperature increases the kinetic energy of liquids and makes them evaporate easily. Low humidity levels allow more evaporation because there is more space in the air to be filled by vapor.

PCM-B shows no evaporation, except for the most extreme case when the temperature and humidity are 50 °C and 25%, respectively. PCM-B has a low vapor pressure, making it harder to evaporate. The lack of evaporation makes PCM-B a favorable choice over PCM-A.

Table 3. 2. 1 Evaporation of PCMs at different environmental conditions

		% of Initial PCM Mass after 2 Hours											
		Sandy Soil						Glacial Till					
Temperature (°C)	Humidity (%)	A5	A10	A15	B5	B10	B15	A5	A10	A15	B5	B10	B15
25	25	67	73	78	101	101	100	85	76	81	107	103	101
	50	70	72	84	102	102	101	92	85	88	114	107	103
	75	79	82	89	103	102	102	98	93	93	116	109	105
35	25	59	64	63	99	99	100	78	77	77	111	104	102
	50	67	73	75	107	102	101	91	81	84	122	109	106
	75	81	82	84	102	102	101	99	93	94	123	111	107
50	25	35	48	52	96	95	98	64	65	65	120	107	103
	50	47	58	61	105	100	100	79	71	73	123	112	106
	75	63	70	75	107	101	102	94	84	82	138	119	110

GT = Glacial Till; SS = Sandy Soil; A5 = PCM-A at 5%; A10 = PCM-A at 10%; A15 = PCM-A at 15%; B5 = PCM-B at 5%; B10 = PCM-B at 10%; B15 = PCM-B at 15%

The values above 100 suggest that the soil retains moisture from the air. GT specimens retain more humidity from the air than SS does. The charged surface of GT attracts the surrounding particles more strongly than the non-charged sand grains, resulting in higher moisture retention.

3.2.5 Freezing Point Depression Test:

Figure 3.2.4 illustrates the freezing curves for the control specimen, and soils treated with PCM-A, PCM-B, and water. PCM-A freezes between 0°C to 2.2 °C in both types of soil as shown in Figure 3.2.4a and Figure 3.2.4c. PCM-B freezes between 2.8 °C to 6.1 °C in GT and 1.5 °C to 5.0 °C in SS, as indicated in Figure 3.2.4b and Figure 3.2.4d. PCM-A exhibits a significant jump in temperature in SS and GT, except for GT with 5% PCM-A, as illustrated in Figure 3.2.4a and Figure 3.2.4c. The magnitude of these jumps increases with increased PCM-A content.

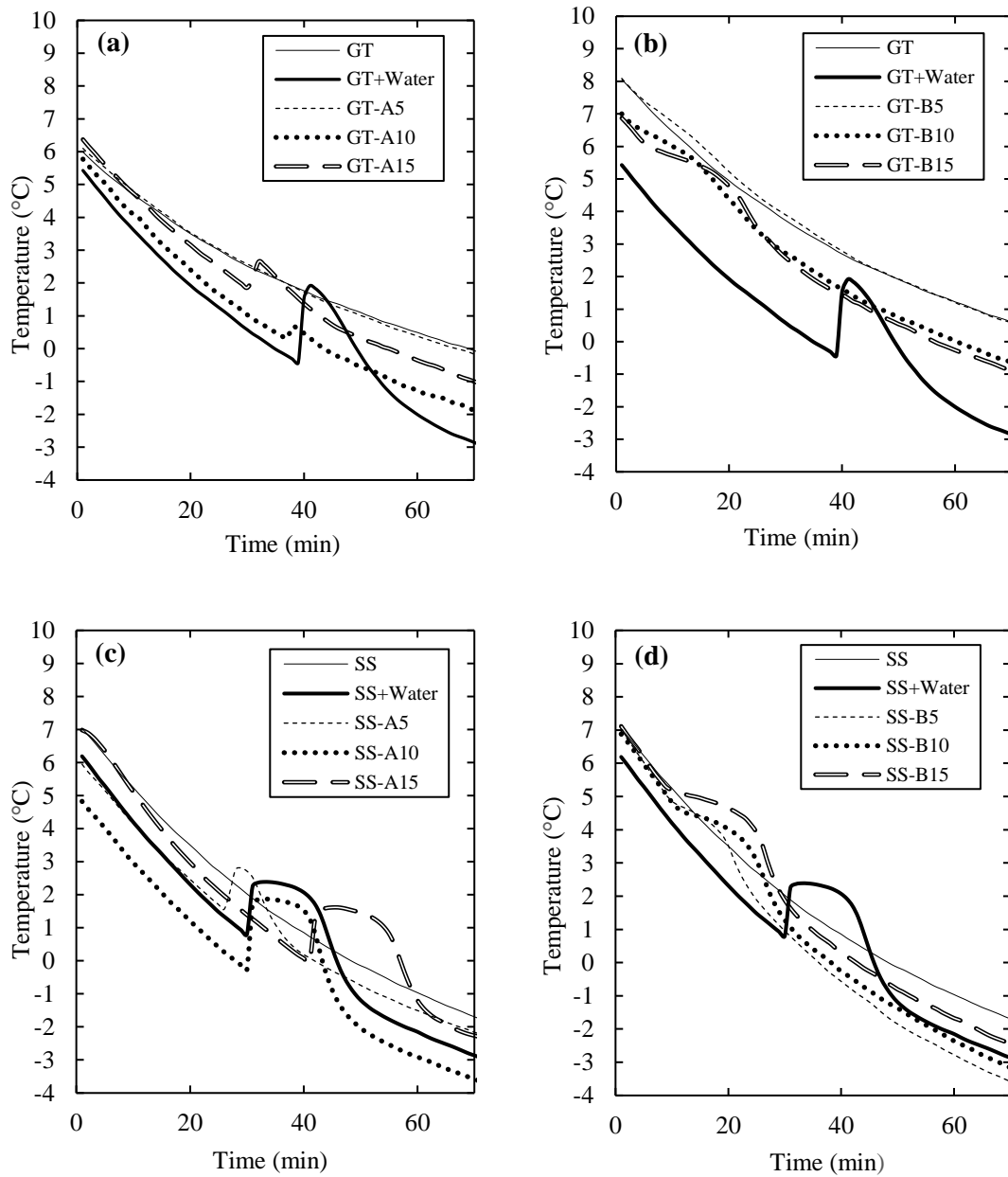


Figure 3. 2. 4 Freezing Point Depression Results of (a) GT with PCM-A, (b) GT with PCM-B, (c) SS with PCM-A, (d) SS with PCM-B

PCM-B does not display a jump like water or PCM-A. Instead, it alters the slope of the curve. This occurs because PCM-B has about half the latent heat of PCM-A, and the latent heat is spread over a temperature range rather than at a single freezing point, which is the case for water. Another observation is that the change in slope becomes more significant as PCM-B content increases, as shown in Figures 3.2.4b and 3.2.4d.

PCM-B freezes before GT-water or SS-water mixture at all PCM-B concentrations. On the other hand, PCM-A does not freeze above the freezing point of water. PCM-A freezes around the same temperature as water. The purpose of the PCM application is to delay the temperature from reaching the freezing point of water. When PCM-A is frozen, some portion of the water will already be frozen inside the soil. Considering this, PCM-B would be more effective at delaying the freezing of soil than PCM-A.

For both PCM-A and PCM-B, the jump or the slope change is smaller in GT compared to SS. This difference might have to do with different specific heat of soils. Sand particles generally have lower specific heat than fine-grained soils. That's why the temperature of SS increases more easily compared to GT.

Soil with pPCM-B did not show any change in curves thus results are not provided. This is because pPCM-B has half the latent heat than that of PCM-B. Consequently, the heat released from pPCM-B was not high enough to be detected by the thermocouples.

3.3 SELECTION OF BEST-PERFORMING PCM AND CONCLUSIONS

Table 3.3.1 summarizes the good and poor properties of each PCM based on characterization tests. PCM-A showed similar results to water, which was attributed to the presence of water in PCM-A. PCM-A exhibited the highest latent heat, as indicated by differential scanning calorimetry (DSC) and freezing point depression test results. It also improved the compaction behavior of SS. However, PCM-A also has high evaporation and expands when frozen, which could cause additional detrimental effects on soils subjected to freeze-thaw cycles.

Even though pPCM-B has low leakage and no evaporation, it has very low latent heat that could not be detected during freezing point depression tests. It dramatically decreases dry unit weight due to its low density. These properties do not make pPCM-B a favorable choice compared to PCM-B.

Table 3. 3. 1 Evaluation for Best-Performing PCM Selection

Properties	PCM-A	PCM-B	pPCM-B
Good	Highest latent heat	Moderate amount of heat Shrinks when frozen No evaporation	Low leakage No evaporation
Poor	High evaporation Expands when frozen Water-based solution	Leakage at higher water and PCM-B contents	Low latent heat Causes a significant reduction in the dry unit weight

PCM-B slightly decreases the dry unit weight of GT while increasing the dry unit weight of SS. Both PCM-A and PCM-B have higher viscosity than water. The higher viscosity is the reason for the better compaction of sand grains. PCM-B showed almost no evaporation, which was a very favorable outcome. Additionally, PCM-B shrinks when frozen, meaning it might not cause a disruptive effect on the soil skeleton, as water expansion does. One drawback of PCM-B is that it leaks out of the soil at high water or PCM-B contents. After consideration of the advantages and disadvantages of each PCM, and assessing information in Table 3.3.1, PCM-B was selected as the best performing PCM and tested for further performance tests: resilient modulus (M_r) and frost-heave and thaw settlement tests.

CHAPTER 4 PERFORMANCE TESTS

4.1 METHODS

Only PCM-B was used for performance tests since it showed the best results in characterization tests. 10% PCM-B content was considered as the optimum concentration. At that concentration, the thermoregulation effect is sufficient, and the leakage occurs to a lesser degree. 15% PCM-B could lead to the leakage issue more easily, and 5% of PCM-B might show weak thermoregulatory impacts. However, due to the high-cost consideration for 10% application, both 5 and 10% of PCM-B were tested for frost-heave and thaw settlement test. Only 10% PCM content was used for the resilient modulus (M_r). The water content was kept constant at 10% for all specimens.

Regarding the dry unit weight values of samples, the dry unit weight of control samples and soil-PCM mixtures was determined based on the Proctor compactor test (ASTM D698-12) and the leakage of PCM-B. The dry unit weight was lowered to prevent PCM-B leakage, if necessary. Duplicate samples were used for each specimen type. Control specimens in SS had a dry unit weight of 17.12 kN/m³, while control specimens in GT had a dry unit weight of 14.77 kN/m³. SS-PCM mixtures had a dry unit weight of 16.18 kN/m³, while GT-PCM mixtures had a dry unit weight of 14.77 kN/m³.

4.1.1 Resilient Modulus Test:

The impact of PCM-B on the resilient modulus (M_r) of soils serves as important complementary data to the frost heave and thaw weakening test. Even if frost action was mitigated by PCM-B, low stiffness caused by PCM-B addition would render it unfavorable.

A triaxial test setup was used to measure the M_r of specimens in accordance with AASTHTO T307. Control specimens and soil-PCM mixtures were subjected to 0, 2, and 5 freeze-thaw cycles before testing. Each cycle had 24 hours of freezing at -23 °C and 23 hours of melting at room temperature (21 °C).

Based on the guidelines provided in NCHRP01-28A, the dimensions of the specimens were selected as 102 mm in diameter and 203 mm in height. The specimens were compacted in six equal layers at 10% water and 10% PCM-B, and the target dry unit weight values. Two latex membranes were used in case one of the membranes was punctured during the experiment. After compacting each layer, the surface was disturbed to provide continuity between layer boundaries. Porous stone and filter paper were placed at the top and bottom of specimens to ensure water drainage and

prevent soil erosion. Then, the specimen was placed in a triaxial chamber, which was sealed with screws and bolts to prevent any confining pressure leakage. The vertical loading and confining pressure sequence are applied following values outlined for subgrade soil in AASTHTO T307, and shown in Table 4.1.1. Drainage was allowed during the testing. Displacements were measured by using external LVDT, whose range was ± 2.54 cm.

Table 4. 1. 1 Load Sequence of Subgrade Soil for Resilient Modulus (M_R) Test (AASHTO T307)

Sequence No.	Confining Pressure, σ_c (kPa)	Deviatoric Stress, $\Delta\sigma$ (kPa)	Number of Load Applications
0	41.4	24.8	500
1	41.4	12.4	100
2	41.4	24.8	100
3	41.4	37.3	100
4	41.4	49.7	100
5	41.4	62.0	100
6	27.6	12.4	100
7	27.6	24.8	100
8	27.6	37.3	100
9	27.6	49.7	100
10	27.6	62.0	100
11	13.8	12.4	100
12	13.8	24.8	100
13	13.8	37.3	100
14	13.8	49.7	100
15	13.8	62.0	100

4.1.2 Frost-Heave and Thaw Settlement Test:

Frost heaving and thaw weakening test for the control and GT-PCM-B mixtures was conducted using the standards outlined in ASTM D5918. No saturation was applied to the specimens. The diameter of the specimens was 146 mm, and the height was 152 mm. A latex membrane was stretched over six acrylic rings in the mold. The acrylic rings and membrane were used for confinement purposes. Oven-dried soils were compacted in six layers at the target PCM-B content, water content, and dry density values inside the acrylic rings.

Porous stones and filter papers were placed at the top and bottom of the specimens to allow water drainage and prevent soil erosion. One heat exchange plate, underlying a surcharge plate

weighing 5 kg, was placed above the top porous stone. Additionally, a bottom heat exchange plate was placed below the base plate. The heat exchange plates served as sources of freezing and thawing temperatures during the experiment. Heat exchange plates were connected to two circulating baths that can have a temperature range between -30 °C and 200 °C. By adjusting the temperature of the circulating bath, the heat exchange plates could apply different temperatures from the top and bottom of the soil. The heat rate capacity of the circulating bath was 505 Watts. Tapes were wrapped around the hoses of the circulating baths to minimize heat loss. The specimens were also covered with insulating material to minimize heat exchange between the specimen and the surrounding space. The temperature schedule for the circulating bath is shown in Table 4.1.2. Mariotte bottles filled with water were placed next to the specimens and connected to base plates. Mariotte bottles provided a constant pressure head of 13 mm with respect to the bottom of the specimens, causing water flow during the experiment. This simulated the water supply needed for frost action. The test was started and carried out by changing the top and bottom exchange plates according to the schedule provided in Table 4.1.2. Specimens were subjected to two freeze-thaw cycles. The specimens started with an initial conditioning temperature of 3.0 °C. Then, they were exposed to 2 freeze-thaw cycles, with each cycle lasting 48 hours—24 hours of freezing and 24 hours of thawing. Each freezing and thawing cycle had two temperature schedules where the top and bottom plates were at two different freezing or melting temperatures. The temperature of the freezer was kept at 4.0 °C during the experiment. Six T-type thermocouples were inserted into the specimens at 6 points with 2.5 cm intervals through the height of the specimens to measure temperature data with depth. Frost heaving and thaw settlement were measured via laser sensors called OptoNCDT 1750 from MicroEpsilon that had a range of 51 mm. Thermocouples and laser sensors were connected to CR1000X data logger and AM16/32B multiplexer for data acquisition. The data were processed using PC400 software, and the results were obtained on PC400. Heaving and temperatures were recorded in real-time.

Table 4. 1. 2 Testing Schedule for frost-heave and thaw settlement test

Start (h)	Finish (h)	Top Plate Temperature (°C)	Bottom Plate Temperature (°C)	Period
0	24	3	3	Conditioning
24	32	-3	3	1st Freezing
32	48	-12	0	
48	64	12	3	1st Thawing
64	72	3	3	
72	80	-3	3	2nd Freezing
80	96	-12	0	
96	112	12	3	2nd Thawing
112	120	3	3	

4.2 RESULTS

4.2.1 Resilient Modulus Test:

Figure 4.2.1 compares the resilient modulus (M_r) values of the specimens subjected to 0,2 and 5 F-T cycles in control specimens (GT) and GT-PCM mixtures. The dashed enclosed areas show the confining pressures applied for each point, which is shown in Table 4.1.1. In GT specimens, as shown in Figure 4.2.1a, there is a significant decrease of about 30% in M_r after 2 freeze-thaw (F-T) cycles. However, between the 2nd and the 5th freeze-thaw cycle, there is no further reduction in M_r . After the 2nd F-T cycle, the larger pore space was then present in the soil due to the effect of the water expansion upon the first two freezing periods. The expansion of water initially disturbed the soil skeleton, reduced M_r , and caused larger pore size. Chamberlain & Gow (1979) also found that F-T cycles increase the permeability of fine-grained soils, which can be correlated to the larger pore size. That is why after 2 F-T cycles, water can freely expand into the larger pore space during freezing, and not affect the soil skeleton. Also, 10% moisture content can be considered low, and it expands in a small amount by volume. Hence, there is no change after 2 F-T cycles.

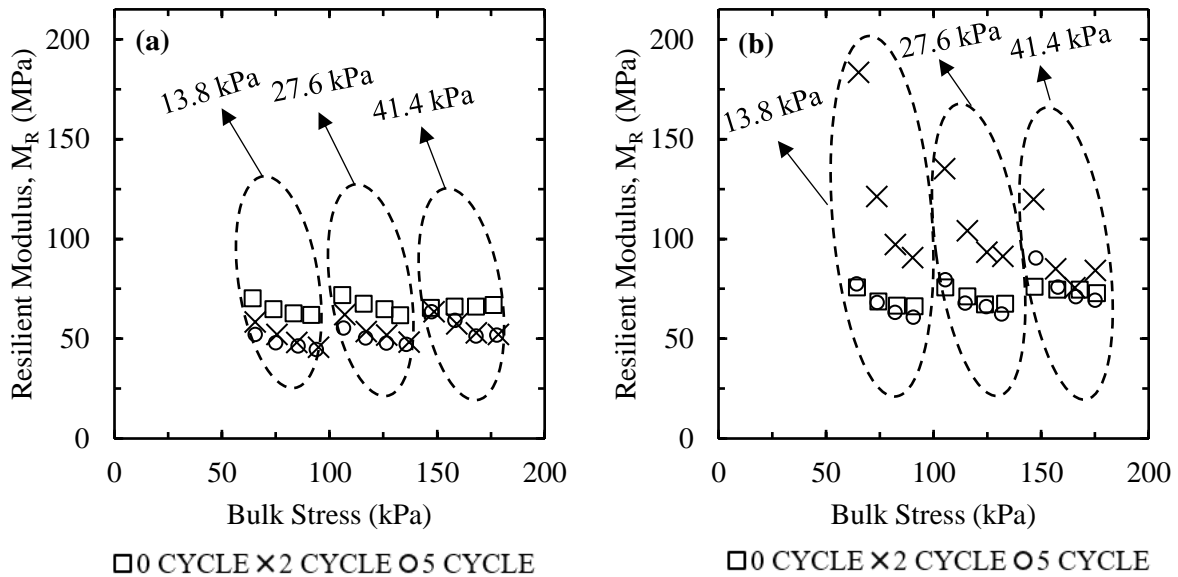


Figure 4. 2. 1 Resilient Modulus of (a) GT (b) GT with 10% PCM-B (GT-B10) at 0, 2 and 5 Freeze-Thaw Cycles

The comparison between GT specimens and GT-PCM mixture at each cycle separately is illustrated in Figure 4.2.2. GT-PCM mixture has the same M_r value at 0 F-T cycle as the GT specimen, possibly due to their identical dry unit weights. After 2 F-T cycles, M_r of the GT-PCM mixture increases significantly, compared to the reduction of M_r in GT specimens. Following 5 F-T cycles, the M_r of GT-PCM mixture returns to the initial value at 0 F-T cycle, whereas the M_r of the GT specimens remains the same as the value after 2 F-T cycles.

PCM-B shrinks about 4% by volume during freezing while water expands. The shrinkage of PCM-B could cause the soil structure to be stiffer due to adhesion forces between the soil and the frozen PCM-B after 2 F-T cycles. However, a stiffer soil structure could be more easily disturbed by water expansion, leading to a reduction after 5 F-T cycles. The two factors, the shrinkage of PCM and the expansion of water counteract each other and could cause fluctuations in the M_r values. The primary conclusion from Figure 4.2.2 is that at any number of freeze-thaw cycles, the GT-PCM mixture has an equal or higher value than GT specimens. Thus PCM-B has no adverse effect on the stiffness of GT.

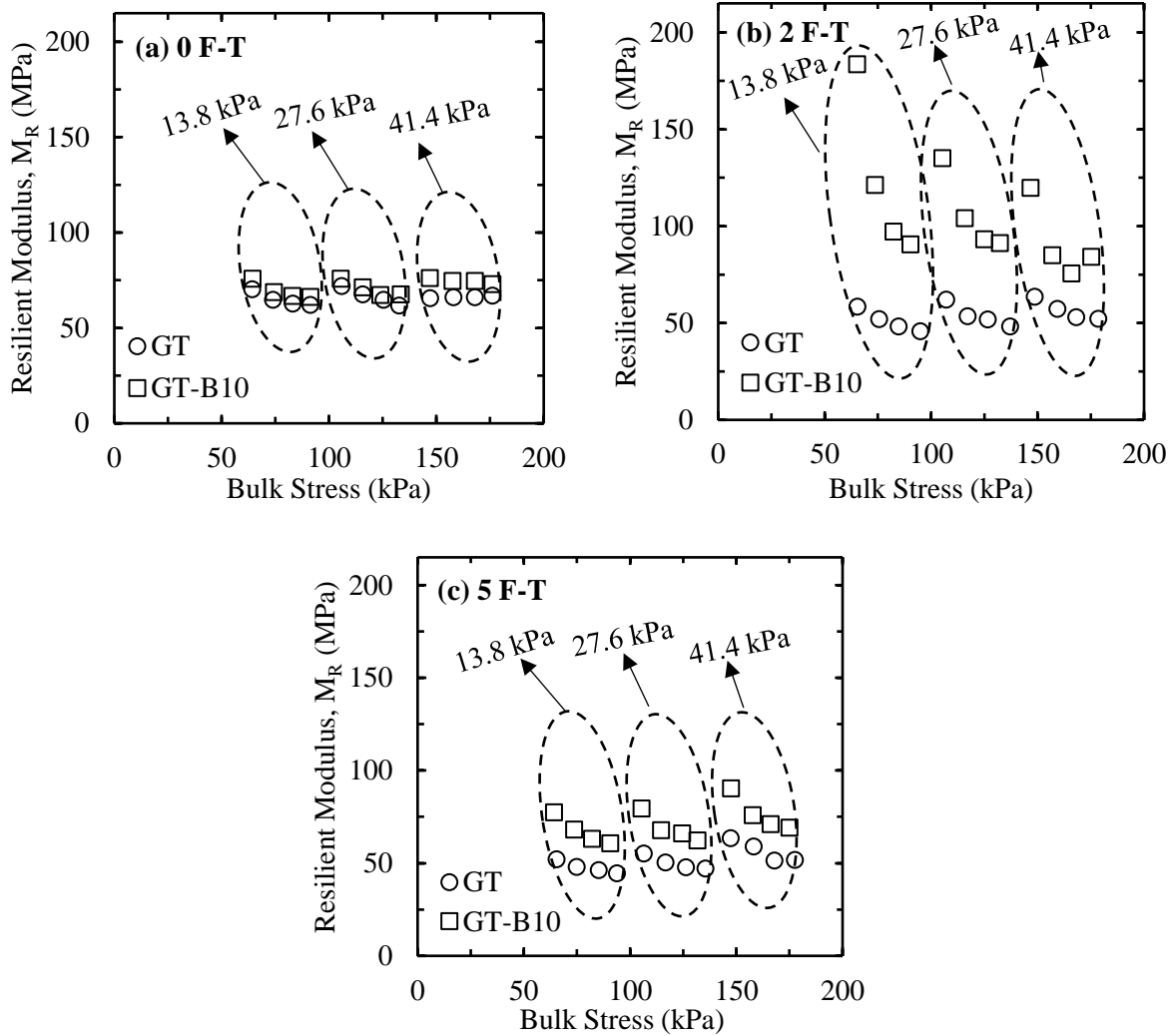


Figure 4. 2. 2 Resilient Modulus of GT and GT with 10% PCM-B (GT-B10) at (a) 0 Freeze-Thaw Cycle (b) 2 Freeze-Thaw Cycle and (c) 5 Freeze-Thaw Cycle

Figure 4.2.3 displays the M_r of SS and SS with 10% PCM-B. SS specimen exhibits a higher M_r value than the SS-PCM mixture at all cycles, which is attributed to the higher dry unit weight of the GT specimen. The reason for the low dry unit weight for SS-PCM mixture was to prevent PCM-B leakage. Achieving a higher dry unit weight and a higher M_r value could be possible by lowering PCM-B content to avoid leakage issues.

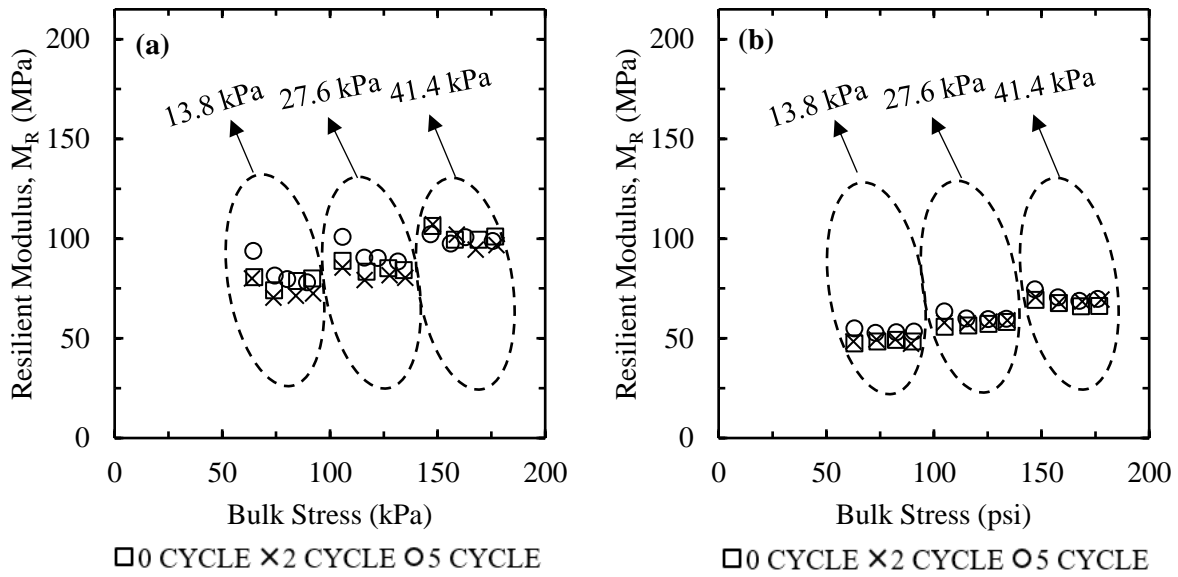


Figure 4. 2. 3 Resilient Modulus of (a) SS (b) SS with 10% PCM-B (SS-B10) at 0, 2 and 5 Freeze-Thaw Cycles

As shown in Figure 4.2.4, no change in the M_r value was observed for either control specimen (SS) or SS-PCM mixtures after 2 and 5 F-T cycles. Similarly, Christ et al. (2009) didn't find a significant change in the dynamic elastic modulus of SS after 10 F-T cycles. The large size pores in the soil structure of sand grains provide enough space for the expansion of 10% water content without disturbing the surrounding soil skeleton. In contrast to GT, the shrinkage of PCM-B does not affect M_r of SS. Due to the absence of electrical charge on the surface of sand grains, PCM-B attaches to the sand grains via a weak adhesion force. Although this adhesion force induces some friction between PCM-B and sand grains during PCM-B shrinkage, it is insufficient to significantly impact the stiffness of the sand grains during F-T cycles.

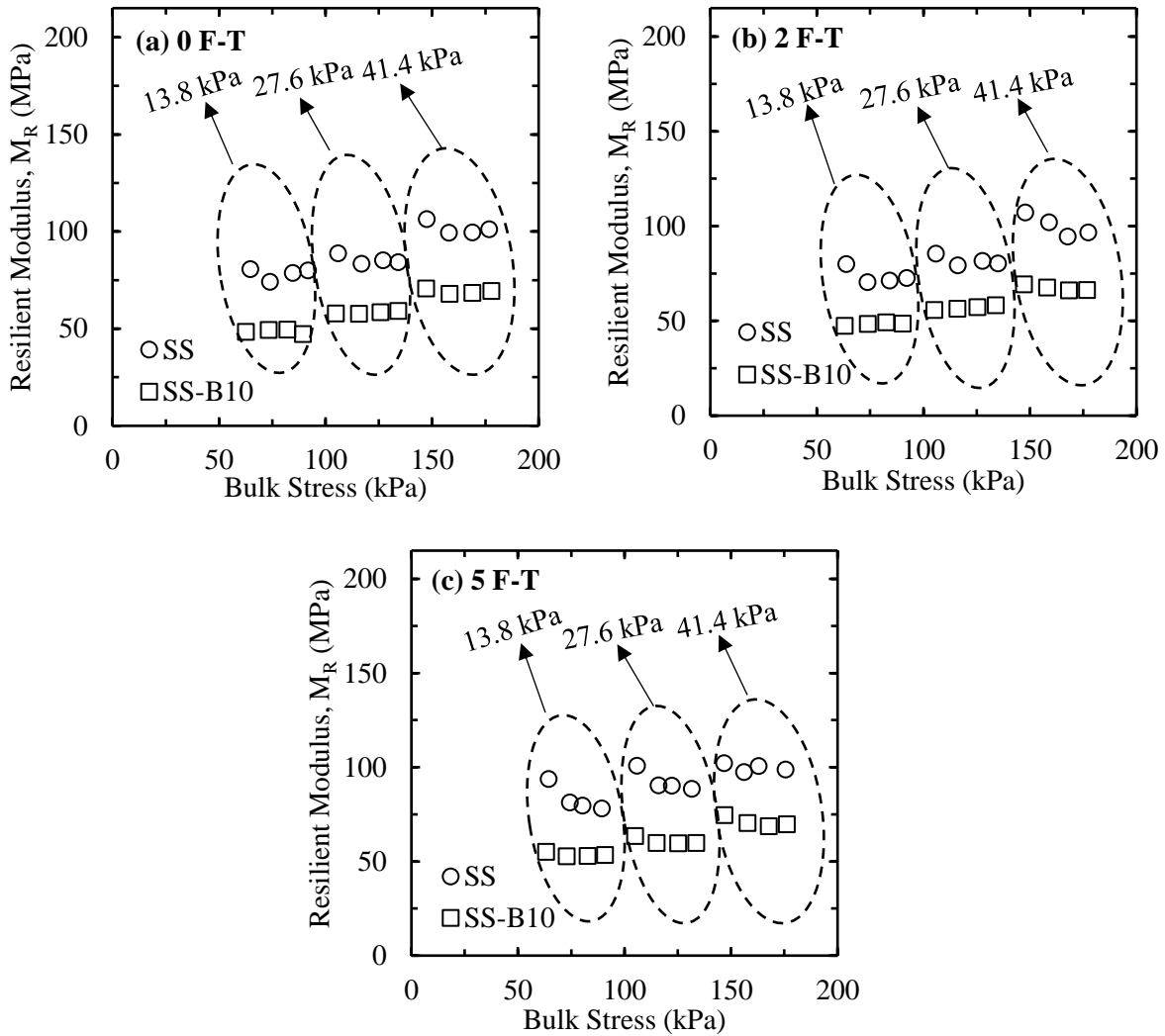


Figure 4. 2. 4 Resilient Modulus of SS and SS with 10% PCM-B (SS-B10) at (a) 0 Freeze-Thaw Cycle (b) 2 Freeze-Thaw Cycle and (c) 5 Freeze-Thaw Cycle

4.2.2 Frost-Heave and Thaw Settlement Test:

Figure 4.2.5 displays the amount of heave with time in GT and GT-PCM samples. All specimens exhibited heaving during the conditioning period when temperatures were above freezing. This was related to the water flowing to the specimen due to the constant head difference of 13 mm provided by the Mariotte bottle, and also GT being expansive soil. Expansive soils increase in volume when the water content increases. Another observation in the conditioning period was that the control specimen exhibited more heaving than the GT-PCM mixture.

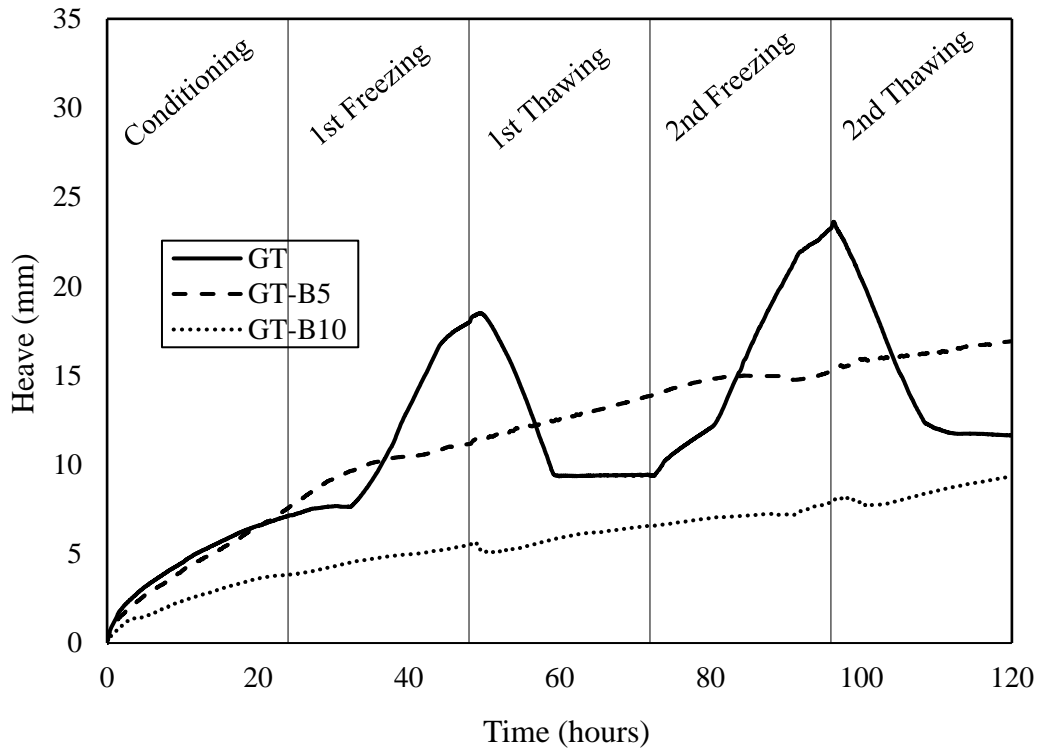


Figure 4. 2. 5 Frost-heave time plot for GT, GT with 5% PCM-B (GT-B5), and GT with 10% PCM-B (GT-B10)

When the conditioning period was over, GT showed the typical heaving and thaw settlement pattern seen in frost susceptible soils. As opposed to that, GT-PCM mixtures displayed a gradual but steady increase in heaving, irrespective of conditioning, freezing, or thawing periods. This observation suggests that frost action did not occur significantly because no extra heaving was observed during the freezing periods. The small frost penetration depth and the presence of frozen PCM-B can cause this result. Frozen PCM-B could have reduced the hydraulic conductivity of soil by narrowing pore spaces during both conditioning and F-T cycles, resulting in less water migration reaching higher depths. Frozen liquids can cause this effect. Artificial ground freezing (AGF) is also a method to reduce seepage and hydraulic conductivity of soils using ice's impenetrable character (Alzoubi et al., 2019). Similarly, Liu & Xie (2012) also stated that an increase in ice content causes a sharp decline in soil permeability. Less water retention was also observed in the unfrozen soil during the conditioning. At that period, some portions of PCM-B were frozen, and some were unfrozen. It is possible that liquid PCM-B decreases the permeability of soil in both states, but the suction pressure causing upward water movement was developed during the freezing period when PCM-B was frozen.

Table 4.2.1 shows the frost penetration depth for the control (GT) and soil-PCM mixture (GT-B10). The values were based on taking 0 °C as the freezing point of the soil, and they represent the average values taken from duplicate samples. GT-B10 had a 44 mm frost penetration depth, which is about half of the frost penetration depth of the control specimen, 95 mm. GT-B5 also had a frost penetration depth of 63 mm, somewhere between the control specimen and GT-B10. The reduction in frost penetration depth was significant, showing the impact of the latent heat released by PCM-B.

Table 4. 2. 1 Frost Penetration Depth of GT, GT with 5% PCM-B (GT-B5), and GT with 10% PCM-B (GT-B10) specimens

Soils	GT	GT-B5	GT-B10
Frost Penetration Depth (mm)	95	63	44

Figure 4.2.6 shows temperatures recorded at different depths for the control (GT) and GT-PCM mixtures (GT-B5 and GT-B10). During freezing, GT-PCM mixtures had a higher temperature than the control specimen at all depths and times. Similarly, Mahedi et al. (2019) and Kravchenko et al. (2020) showed that PCM-treated specimens maintained higher temperatures than the control specimen during F-T cycles. Additional latent heat coming from PCM-B caused the higher temperature values. In this regard, 10% PCM-B was more effective than 5% PCM-B at keeping the temperature higher.

As shown in Table 4.2.1, at depths below 63 mm and 44 mm, water did not freeze in PCM-B5 and PCM-B10, respectively. However, water did freeze up to 95 mm depth in control specimens. Therefore, control specimens utilized additional latent heat of water resulting from increased frost penetration depth and a higher amount of water accumulation in the frozen region due to frost action. This caused the control and PCM-treated specimens to have very close temperature values at lower depths.

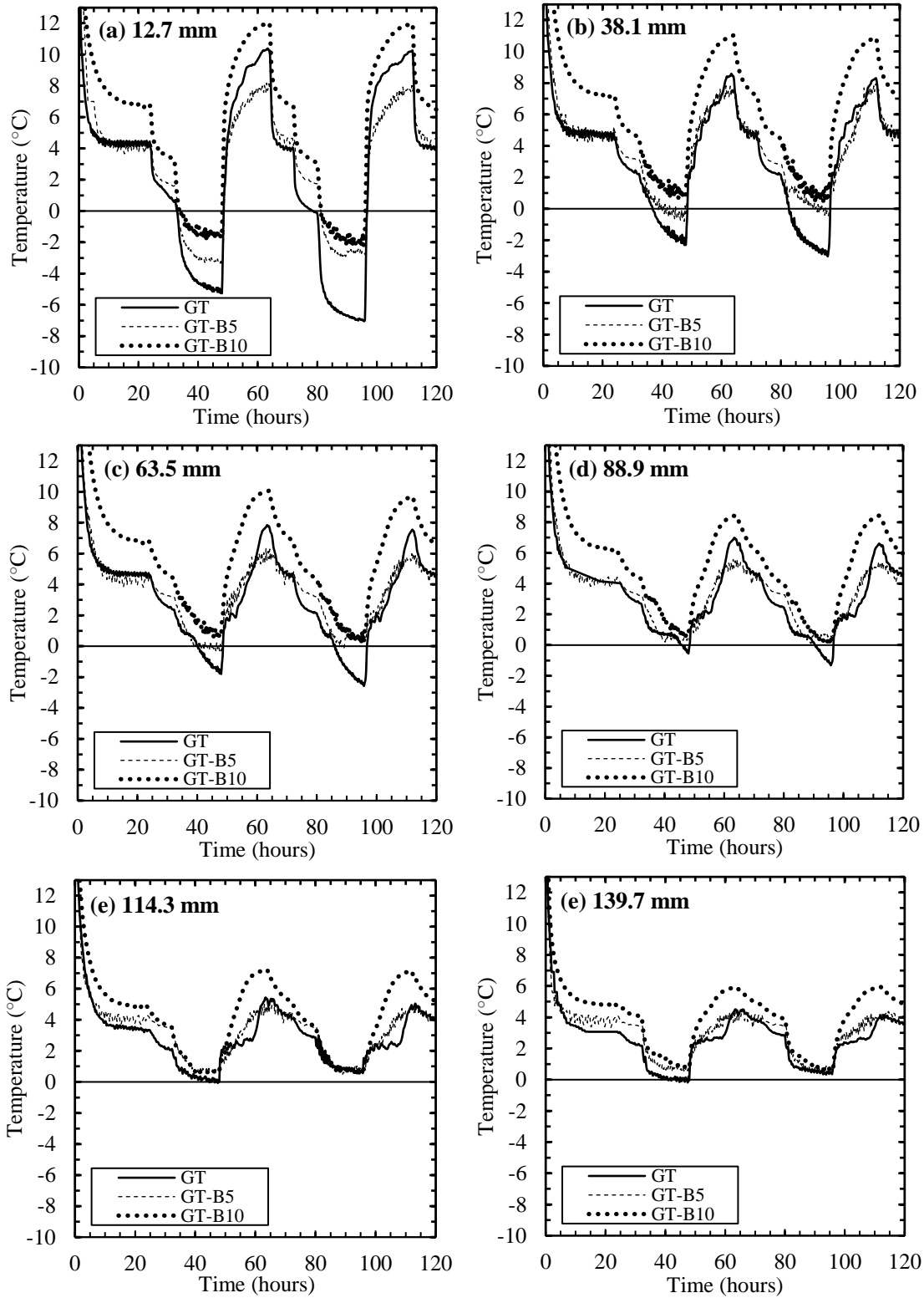


Figure 4. 2. 6 Temperatures variations at a depth of (a) 12.7 mm, (b) 38.1 mm, (c) 63.5 mm, (d) 88.9 mm, (e) 114.3 mm, and (f) 139.7 mm

GT-B10 mixture did not slow the temperature increase during the thawing period more than the control specimen. That is because the moisture content of the control specimen was increasing due to frost action, resulting in a higher total latent coming from migrated water. The additional latent heat in the control specimen kept the temperature lower during thawing than it would otherwise be. GT-B5 experienced an accumulation of water to some degree, which also caused an increase in its total latent heat. That is why GT with 5% PCM showed the least temperature fluctuations overall. The initial temperature difference during freezing between the GT-B5 and GT-B10 specimens decreased because of the same effect.

Figure 4.2.7 shows the heave/thaw rate, maximum heave, and residual heave values of the control and GT-PCM mixtures. The heave rate and the maximum of the control specimen are much higher than those of the GT-PCM mixtures. As discussed, the difference was attributed to the lower frost penetration depth and the effect of frozen PCM-B, which restricts water migration. The soil-PCM mixtures did not experience a decrease in heaving during the thawing period, as indicated by the negative values in Figure 4.2.7c. This also suggests that heaving did not occur due to the expansion of water; otherwise, melting would cause some settlement.

The residual heave values are close to each other in Figure 4.2.7d. The control specimen had permanent residual heave due to the frost action and also due to the expansive nature of GT. GT-PCM mixtures heaved not because of frost action, but because of the water migration below the frost penetration depth caused by the matric potential of the region with drier soil.

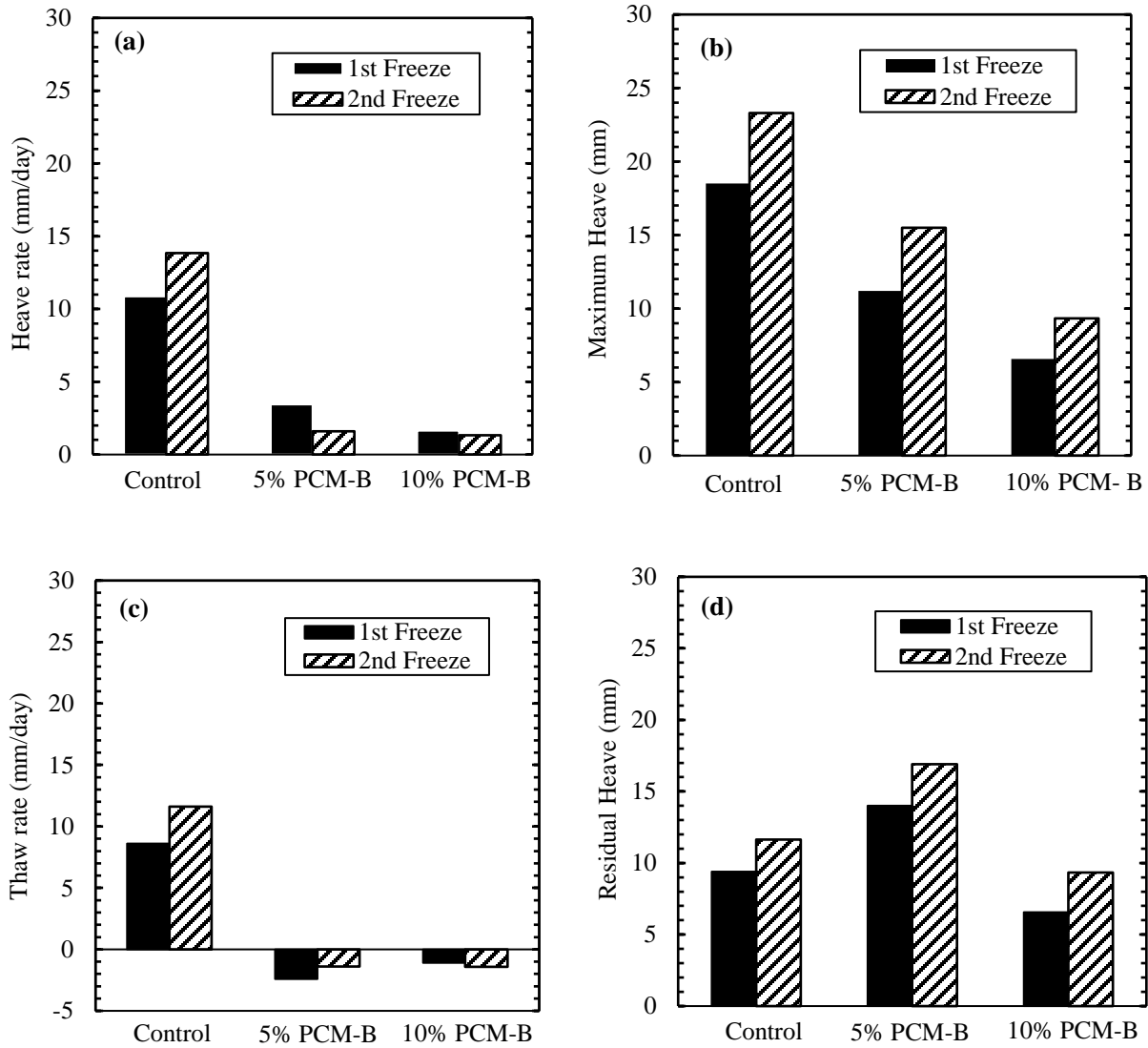


Figure 4. 2. 7 Frost heave and thaw weakening test results of GT, GT with 5% PCM-B (GT-B5), and GT with 10% PCM-B (GT-B10); (a) heave rate, (b) maximum heave, (c) thaw rate, and (d) residual heave

Figure 4.2.8 shows the moisture content versus depth for the control specimen and the GT-PCM mixtures. The control specimen exhibited a slightly decreasing moisture content with increasing depth, while the moisture content was increased significantly with increasing depth in GT-PCM mixtures. Frozen PCM-B restricted the pathways of water migration and lowered the soil permeability. 10% PCM-B was more effective than 5% PCM-B in this aspect. Similarly, the sharp change in moisture around 40-60mm for GT-B5 and GT-B10 is attributed to the additional permeability reduction caused by frozen water, and the low water supply to feed the frozen fringe

caused by the low moisture content. The moisture content still increased below the freezing point of water; due to the matric potential of drier parts of the soil. Finally, the moisture content of the soil-PCM mixtures is lower than the control specimen at all depths, showing successful mitigation of the frost action by PCM-B incorporation in soil.

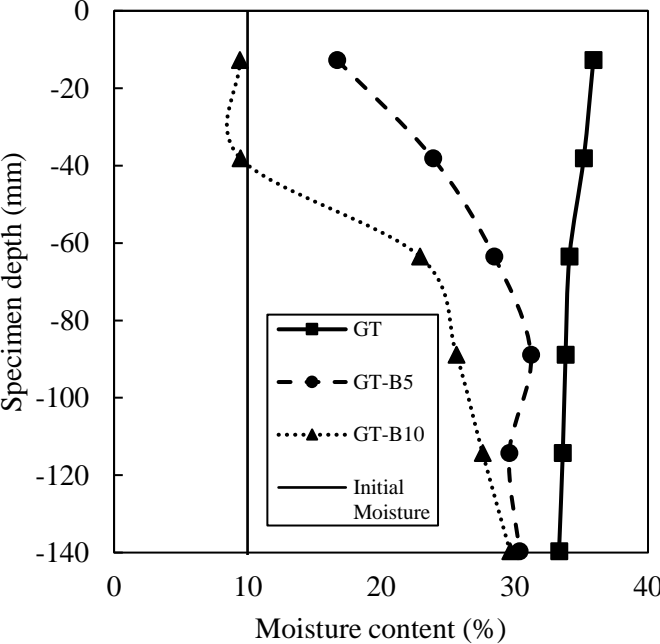


Figure 4. 2. 8 Moisture Profile vs Depth for GT, GT with 5% PCM-B (GT-B5), and GT with 10% PCM-B (GT-B10)

CHAPTER 5 CONCLUSIONS AND RECOMMENDATIONS

Mitigating the effects of frost action is crucial to increase the serviceability and lifespan of roadways in regions experiencing cold winters. Incorporation of PCM into the soil is a viable solution to mitigate the effects of frost action by providing latent heat and minimizing temperature fluctuation near the freezing point of the soil. The selection of the right PCM is crucial for soil application. PCM should undergo a phase change near the freezing point of soil and remain stable over many freeze-thaw cycles. Also, any chemical incorporation into the soil can cause additional beneficial or harmful effects that must be investigated.

5.1 SUMMARY

Three types of PCM were first characterized by differential scanning calorimetry (DSC), Atterberg limits, Harvard compaction test, scanning electron microscope (SEM) imaging, PCM evaporation, and freezing point depression test. PCM-B showed the overall best results for soil application. It demonstrated very little evaporation and a moderate amount of latent heat, and it froze before the freezing point of water which would delay the freezing of soil. Only PCM-B was used for further main performance tests. As part of the main performance tests, PCM-B was tested for its effect on resilient modulus and frost heaving and thaw weakening of soils. The performance tests confirmed that PCM-B was indeed a suitable choice. It caused no reduction in stiffness in GT, exhibited a positive thermoregulation effect by maintaining higher temperatures, and provided an additional barrier against upward water migration caused by frost action via reducing the soil permeability.

5.2 CONCLUSIONS

The key findings from this study are shown below:

- PCM-B was a better application for soil than PCM-A and pPCM-B due to the shrinkage characteristic during freezing and very little to no evaporation at different environmental conditions.
- pPCM-B was found unsuitable for incorporation in soil because it dramatically decreases the dry unit weight and provides little latent heat.
- PCM-A is a salt-based hydrate that contains water, and it expands upon freezing. Incorporating PCM-A might have the same effect as adding additional water to the soil and worsen frost action.

- One drawback of PCM-B is that it leaks at higher PCM or water contents. Water particles try to replace PCM-B, causing leakage of PCM-B. This limits the amount of PCM incorporation in the soil.
- None of the PCMs showed any sign of chemical reactions in SEM images. This suggests that the full latent heat of PCM can be utilized without any PCM loss due to chemical reactions.
- PCM-B caused a higher temperature than the control specimens during freeze-thaw (F-T) cycles, showing a successful thermoregulation effect.
- The latent heat of control specimens can increase more than that of PCM-treated specimens with F-T cycles. That's because control specimens retain water due to frost action, which increases the latent heat potential of the soil. Even though the latent heat capacity increases, this occurs when already significant frost action takes place.
- 5% and 10% PCM-B applications reduced the frost penetration depth by about 35% and 50%, respectively. As a result, the total heave, residual heave, and heave rates were significantly lowered.
- Frozen PCM-B decreased the permeability of the soil, reducing the water migration caused by frost action. 10% PCM-B was more effective than 5% PCM-B in that regard.
- Unfrozen PCMs can also decrease soil permeability by filling up pore spaces. However, the upward water migration tendency in frost action occurs during the freezing period of F-T cycles when PCM-B is frozen. So, the observations are limited to the effect of liquid PCM-B on soil permeability.
- PCM-B did not decrease the resilient modulus (M_r) values after 0, 2, and 5 F-T cycles for both coarse (SS) and fine-grained soil (GT), further making it a suitable PCM choice. The reason could be related to the shrinkage of PCM-B upon freezing, which would not cause any disruption to soil as opposed to the expansion of water.
- In fine-grained soil (GT), PCM-B showed an increase in M_r after 2 F-T cycles and a subsequent decrease after 5 F-T cycles. The shrinkage of PCM and the expansion of water during F-T cycles might have opposite effects on the stiffness and cause fluctuations in M_r values.

- The reduction in M_r for fine-grained soil stopped after the 2nd F-T cycle at a 10% moisture content. This shows that the effect of F-T cycles can stop even as early as the second cycle due to the low moisture content and enlarged pore size by the first two F-T cycles.
- M_r values of control specimen SS and SS-PCM mixtures did not change at 2 and 5 F-T cycles, suggesting that coarser-grained materials are less affected by F-T cycles due to their large pore spaces.

The conclusions show that PCMs are promising solutions to reduce the harmful effects of frost action by providing a thermoregulatory effect on temperature fluctuations. An additional benefit was also seen by the reduced permeability of soil due to frozen PCM-B presence, which slowed down the water migration to upper levels. The results show that PCM-B can help decrease the severity and the number of F-T cycles in subgrade soil.

5.3 RECOMMENDATIONS

Based on the results of this study, the following recommendations are proposed for further research and understanding:

- **Use of other PCMs (water in encapsulated form):** Given that the latent heat of PCM-B successfully resulted in higher temperatures during freeze-thaw (F-T) cycles compared to control specimens, and the frost penetration depth was reduced by about 35 and 50%, it can be concluded that the latent heat energy of any PCM holds promise as a solution to mitigate the damage of F-T cycles in soil. Therefore, other PCMs with better properties (such as higher latent heat and no leakage) can be tested for better performance. If their latent heat can be effectively utilized, better thermoregulation can be achieved. For instance, water has a high latent heat, and water in encapsulated form could be an alternative to the PCMs used in this study.
- **Frozen liquid application in soil:** As demonstrated by this study and artificial ground freezing (AGA) application, frozen liquids can decrease the permeability of soil significantly. The applicability of this concept can be further investigated and expanded by large-scale experiments or by using other chemicals that do not necessarily have high latent heat. Unfrozen liquids can also demonstrate this effect by filling up pore spaces as well. This case was not tested in this study. However, additional research can also focus on that phenomenon.

REFERENCES

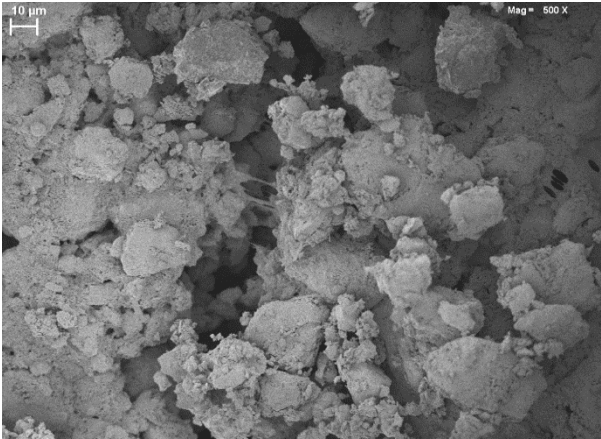
- Alzoubi, M. A., Madiseh, A., Hassani, F. P., & Sasmito, A. P. (2019). Heat transfer analysis in artificial ground freezing under high seepage: Validation and heatlines visualization. <https://doi.org/10.1016/j.ijthermalsci.2019.02.005>
- Anupam, B. R., Sahoo, U. C., & Rath, P. (2020). Phase change materials for pavement applications: A review. *Construction and Building Materials*, 247, 118553. <https://doi.org/10.1016/J.CONBUILDMAT.2020.118553>
- Cabeza, L. F., Castell, A., Barreneche, C., De Gracia, A., & Fernández, A. I. (2011). Materials used as PCM in thermal energy storage in buildings: A review. *Renewable and Sustainable Energy Reviews*, 15, 1675–1695. <https://doi.org/10.1016/j.rser.2010.11.018>
- Carter, M., & Bentley, S. P. (2016). *Soil Properties and their Correlations (Second Edition)*. John Wiley & Sons.
- Castell, A., Martorell, I., Medrano, M., Pérez, G., & Cabeza, L. F. (2010). Experimental study of using PCM in brick constructive solutions for passive cooling. *Energy and Buildings*, 42(4). <https://doi.org/10.1016/j.enbuild.2009.10.022>
- Cetin, B., Ashlock, J., & Jahren, C. (2019). Performance-Based Evaluation of Cost-Effective Aggregate Options for Granular Roadways.
- Chamberlain, E. J., & Gow, A. J. (1979). EFFECT OF FREEZING AND THAWING ON THE PERMEABILITY AND STRUCTURE OF SOILS. *Engineering Geology*, 13, 73–92.
- Chen, M., Wan, L., & Lin, J. (2012). Effect of phase-change materials on thermal and mechanical properties of asphalt mixtures. *Journal of Testing and Evaluation*, 40(5). <https://doi.org/10.1520/JTE20120091>
- Christ, M., Kim, Y. C., & Park, J. B. (2009). The influence of temperature and cycles on acoustic and mechanical properties of frozen soils. *KSCE Journal of Civil Engineering*, 13(3), 153–159. <https://doi.org/10.1007/s12205-009-0153-1>
- Coban, H. S., & Cetin, B. (2022). Suitability Assessment of Using Lime Sludge for Subgrade Soil Stabilization. *Journal of Materials in Civil Engineering*, 34(3). [https://doi.org/10.1061/\(asce\)mt.1943-5533.0004122](https://doi.org/10.1061/(asce)mt.1943-5533.0004122)
- De Matteis, V., Cannavale, A., Martellotta, F., Rinaldi, R., Calcagnile, P., Ferrari, F., Ayr, U., & Fiorito, F. (2019). Nano-encapsulation of phase change materials: From design to thermal performance, simulations and toxicological assessment. *Energy & Buildings*, 1–11. <https://doi.org/10.1016/j.enbuild.2019.02.004>
- DiMillio, A. F. (1999). *A Quarter Century of Geotechnical Research, Chapter 4: Soil and Rock Behavior*.
- Doré, G. (2004). Development and validation of the thaw-weakening index. *International Journal of Pavement Engineering*, 5(4), 185–192. <https://doi.org/10.1080/10298430412331317464>
- Dore, G. (2020). Frost Action in Soils Fundamentals and Mitigation in a Changing Climate: CHAPTER 8 Mitigation of Frost Action. American Society of Civil Engineers (ASCE).

- Farnam, Y., Esmaeeli, H. S., Zavattieri, P. D., Haddock, J., & Weiss, J. (2017). Incorporating phase change materials in concrete pavement to melt snow and ice. *Cement and Concrete Composites*, 84, 134–145.
- Farnam, Y., Krafcik, M., Liston, L., Washington, T., Erk, K., Tao, B., & Weiss, J. (2016). Evaluating the Use of Phase Change Materials in Concrete Pavement to Melt Ice and Snow. *Journal of Materials in Civil Engineering*, 28(4). [https://doi.org/10.1061/\(asce\)mt.1943-5533.0001439](https://doi.org/10.1061/(asce)mt.1943-5533.0001439)
- Fleischer, A. S. (2015). *Thermal Energy Storage Using Phase Change Materials*.
- Hawe, D. W., Banu, D., & Feldman, D. (1989). Latent heat storage in concrete. *Sol. Energy Mater.*, 19(3), 335–348.
- Henry, K. S., & Holtz, R. D. (2001). Geocomposite capillary barriers to reduce frost heave in soils. *Canadian Geotechnical Journal*, 38(4), 678–694. <https://doi.org/10.1139/cgj-38-4-678>
- Hoekstra, P. (1969). Water Movement and Freezing Pressures. *Soil Science Society of America Journal*, 33(4), 512–518. <https://doi.org/10.2136/SSSAJ1969.03615995003300040011X>
- Huang, X., Chen, X., Li, A., Atinafu, D., Gao, H., Dong, W., & Wang, G. (2018). Shape-stabilized phase change materials based on porous supports for thermal energy storage applications. <https://doi.org/10.1016/j.cej.2018.09.013>
- Isotalo, J. (1995). SEASONAL TRUCK LOAD RESTRICTIONS: MITIGATING EFFECTS OF SEASONAL ROAD STRENGTH VARIATIONS. IXTH INTERNATIONAL CONFERENCE ON LOW-VOLUME ROADS, 137–141.
- Johnson, A. E. (2012). *Freeze-thaw performance of pavement foundation materials*. Iowa State University.
- Kalnaes, S. E., & Petter Jelle, B. (2015). Phase change materials and products for building applications: A state-of-the-art review and future research opportunities. *Energy and Buildings*, 94, 150–176. <https://doi.org/10.1016/j.enbuild.2015.02.023>
- Kestler, M. A., Berg, R. L., Steinert, B. C., Hanek, G. L., Truebe, M. A., & Humphrey, D. N. (2007). Determining when to place and remove spring load restrictions on low-volume roads: Three low-cost techniques. *Transportation Research Record*, 2(1989), 219–229. <https://doi.org/10.3141/1989-67>
- Kravchenko, E., Liu, J., Chang, D., Rao, Y., & Krainiukov, A. (2020). Study of the thermal field of a mixture of soil and PCM materials with simulation of the warming effect during a phase change. *Construction and Building Materials*, 262. <https://doi.org/10.1016/j.conbuildmat.2020.120818>

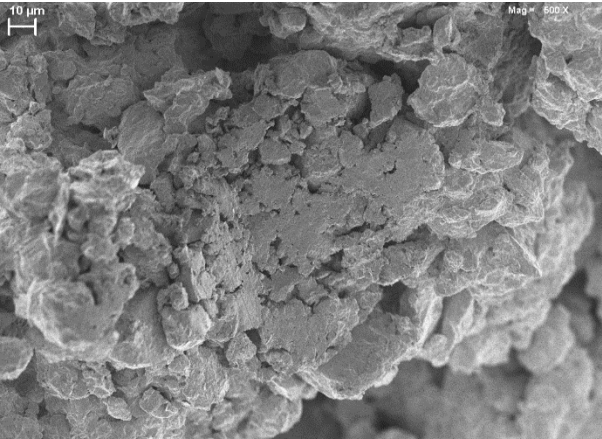
- Levinson, D., Marasteanu, M., Voller, V., Margineau, I., Smalkoski, B., Hashami, M., & Li, N. (2005). 4. Title and Subtitle 5. Report Date Spring Load Restrictions Pavement effects Road damage. <http://www.lrrb.org/PDF/200515.pdf>
- Li, S., Lai, Y., Pei, W., Zhang, S., & Zhong, H. (2014). Moisture-temperature changes and freeze-thaw hazards on a canal in seasonally frozen regions. *Natural Hazards*, 72(2), 287–308. <https://doi.org/10.1007/s11069-013-1021-3>
- Liu, J., & Xie, J. (2012). Nonlinear analyses for the permeability coefficient of frozen soil. *Electron. J. Geotech. Eng.*, 17, 3875–3886.
- Ma, B., Wang, S., & Li, J. (2011). Study on application of PCM in asphalt mixture. *Advanced Materials Research*, 168–170, 2625–2630. doi.org/10.4028/www.scientific.net/AMR.168-170.2625
- Mahedi, M., Cetin, B., & Cetin, K. S. (2019). Freeze-thaw performance of phase change material (PCM) incorporated pavement subgrade soil. *Construction and Building Materials*, 202, 449–464. <https://doi.org/10.1016/j.conbuildmat.2018.12.210>
- Miller, R. D. (1972). Freezing and heaving of saturated and unsaturated soils. *Highw. Res. Rec.*, 393, 1–11.
- Naqvi, M. W., Sadiq, Md. F., Cetin, B., Uduebor, M., & Daniels, J. (2023). Frost Susceptibility Evaluation of Clay and Sandy Soils. 455–465. <https://doi.org/10.1061/9780784484678.046>
- Oflaherty C.A., & Andrews, D. C. (1968). Frost effects in lime and cement-treated soils. *Highway Research Record*.
- Rempel, A. W. (2007). Formation of ice lenses and frost heave. *Journal of Geophysical Research: Earth Surface*, 112(2). <https://doi.org/10.1029/2006JF000525>
- Sadiq, M. F., Naqvi, M. W., Cetin, B., & Daniels, J. (2023). Role of Temperature Gradient and Soil Thermal Properties on Frost Heave. *Transportation Research Record: Journal of the Transportation Research Board*, 036119812211472. <https://doi.org/10.1177/03611981221147261>
- Sharma, A., Tyagi, V. V, Chen, C. R., & Buddhi, D. (2009). Review on thermal energy storage with phase change materials and applications. <https://doi.org/10.1016/j.rser.2007.10.005>
- Sheng, D., Zhang, S., Yu, Z., & Zhang, J. (2013). Assessing frost susceptibility of soils using PCHeave. <https://doi.org/10.1016/j.coldregions.2013.08.003>
- Si, W., Zhou, X. Y., Ma, B., Li, N., Ren, J. P., & Chang, Y. J. (2015). The mechanism of different thermoregulation types of composite shape-stabilized phase change materials used in asphalt pavement. *Construction and Building Materials*, 98, 547–558. <https://doi.org/10.1016/j.conbuildmat.2015.08.038>

- Su, W., Darkwa, J., & Kokogiannakis, G. (2015). Review of solid-liquid phase change materials and their encapsulation technologies. *Renew. Sustain. Energy Rev.* , 48, 373–391.
- Takagi, S. (1979). Segregation Freezing as the Cause of Suction Force for Ice Lens Formation. *Developments in Geotechnical Engineering*, 26(C), 93–100. <https://doi.org/10.1016/B978-0-444-41782-4.50013-0>
- Thomas, H. R., Cleall, P., Li, Y. C., Harris, C., & Kern-Luetschg, M. (2009). Modelling of cryogenic processes in permafrost and seasonally frozen soils. *Geotechnique*, 59(3), 173–184. <https://doi.org/10.1680/GEOT.2009.59.3.173>
- Tiedje, E. (2015). THE EXPERIMENTAL CHARACTERIZATION AND NUMERICAL MODELLING OF FROST HEAVE. McMaster University.
- Tyagi, V. V., Chopra, K., Sharma, R. K., Pandey, A. K., Tyagi, S. K., Ahmad, M. S., Sari, A., & Kothari, R. (2022). A comprehensive review on phase change materials for heat storage applications: Development, characterization, thermal and chemical stability. In *Solar Energy Materials and Solar Cells* (Vol. 234). Elsevier B.V. <https://doi.org/10.1016/j.solmat.2021.111392>
- Wang, X., Zhang, L., Yu, Y. H., Jia, L., Mannan, M. S., Chen, Y., & Cheng, Z. (2015). Nano-encapsulated PCM via Pickering Emulsification. *Scientific Reports*, 5. <https://doi.org/10.1038/srep13357>
- Yeon, J. H., & Kim, K. K. (2018). Potential applications of phase change materials to mitigate freeze-thaw deteriorations in concrete pavement. *Construction and Building Materials*, 177, 202–209. <https://doi.org/10.1016/j.conbuildmat.2018.05.113>
- Zhou, D., Zhao, C. Y., & Tian, Y. (2011). Review on thermal energy storage with phase change materials (PCMs) in building applications. <https://doi.org/10.1016/j.apenergy.2011.08.025>

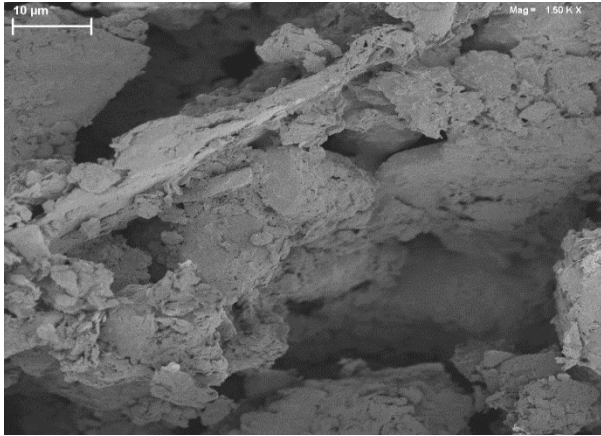
APPENDIX: SEM COMPARISON OF CONTROL AND PCM-TREATED SPECIMENS



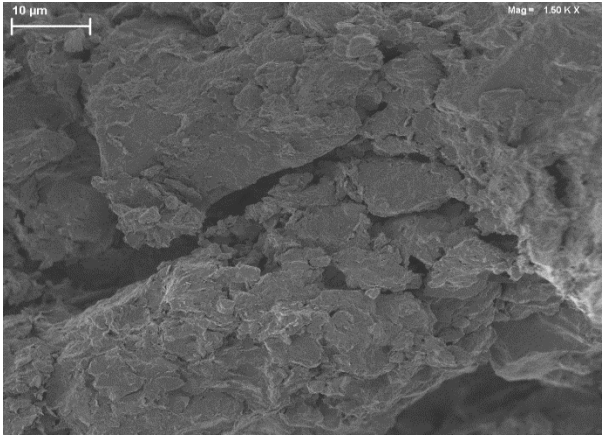
a) GT (Mag: 500x)



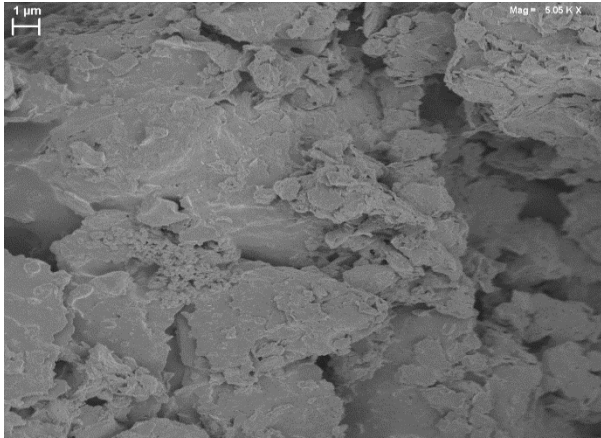
b) GT-A10 (Mag: 500x)



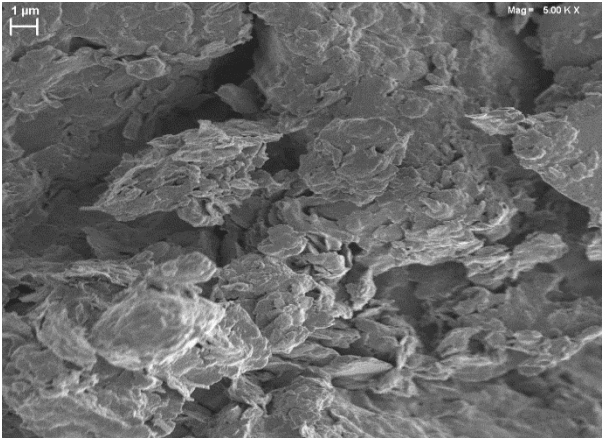
c) GT (Mag: 1500x)



d) GT-A10 (Mag: 1500x)

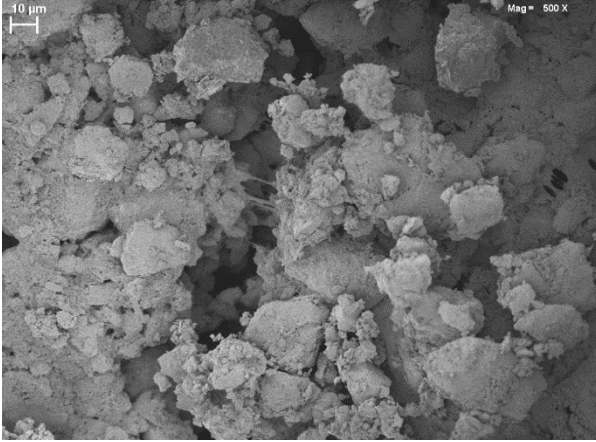


e) GT (Mag: 5000x)

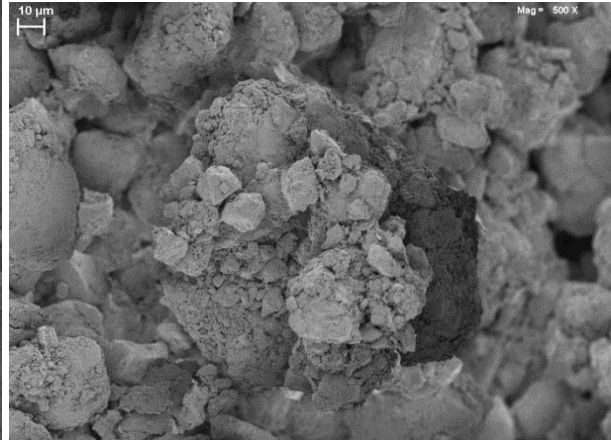


f) GT-A10 (Mag: 5000x)

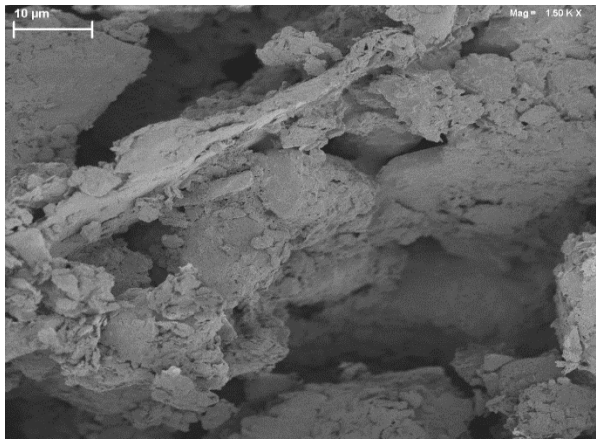
Figure A. 1 SEM image comparison between GT and GT with PCM-A at different magnification values



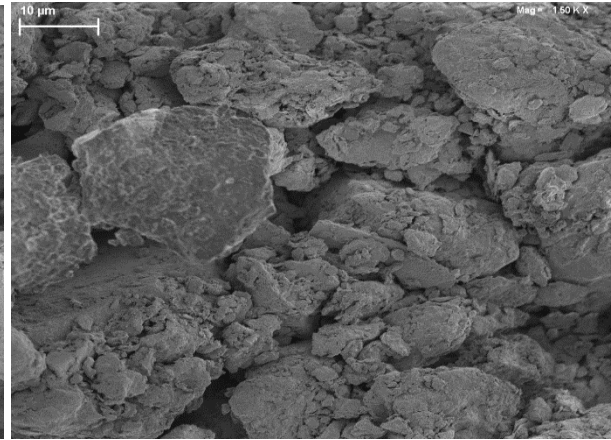
a) GT (Mag: 500x)



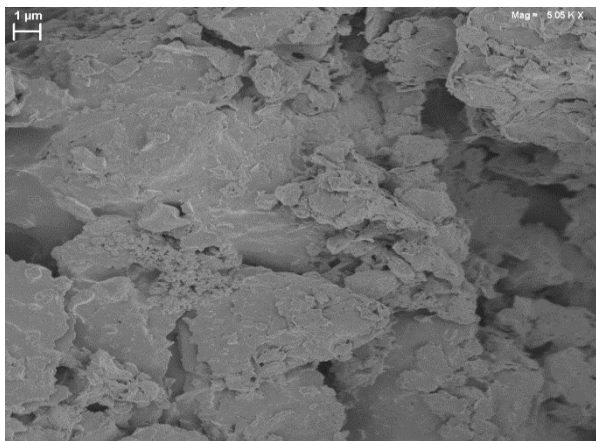
b) GT-B10 (Mag: 500x)



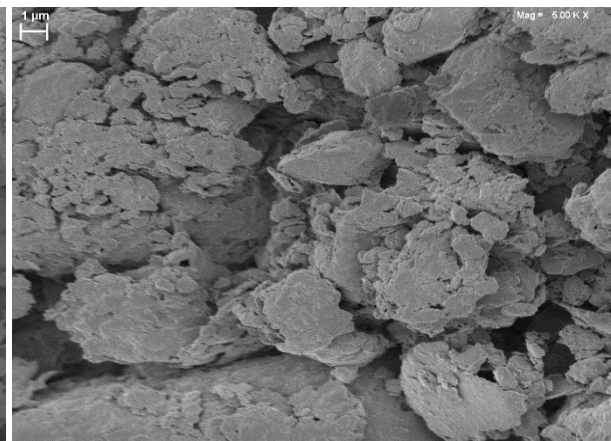
c) GT (Mag: 1500x)



d) GT-B10 (Mag: 1500x)



e) GT (Mag: 5000x)

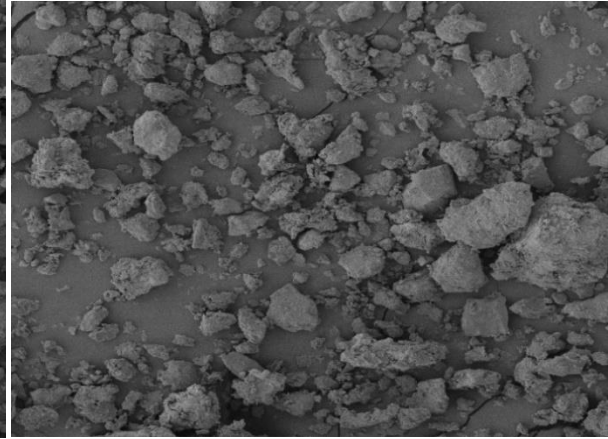


f) GT-B10 (Mag: 5000x)

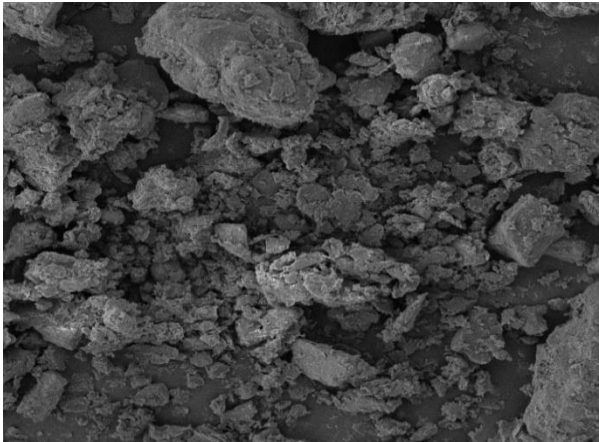
Figure A. 2 SEM image comparison between GT and GT with PCM-B at different magnification values



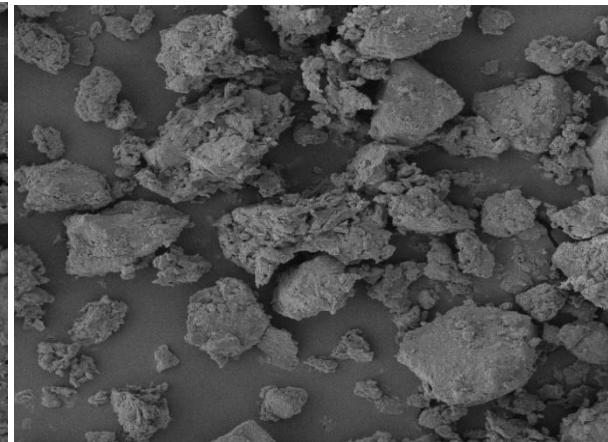
a) GT (Mag: 500x)



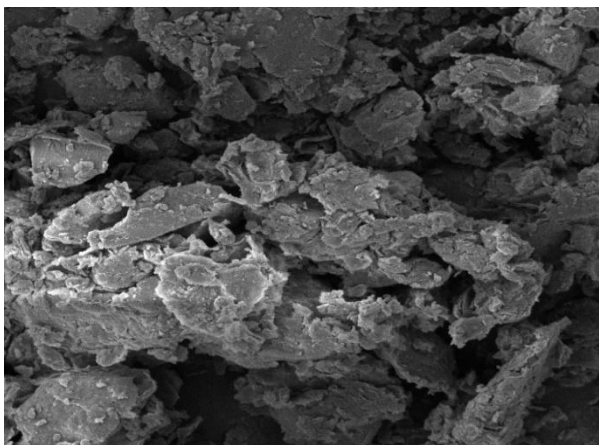
b) GT-pB10 (Mag: 500x)



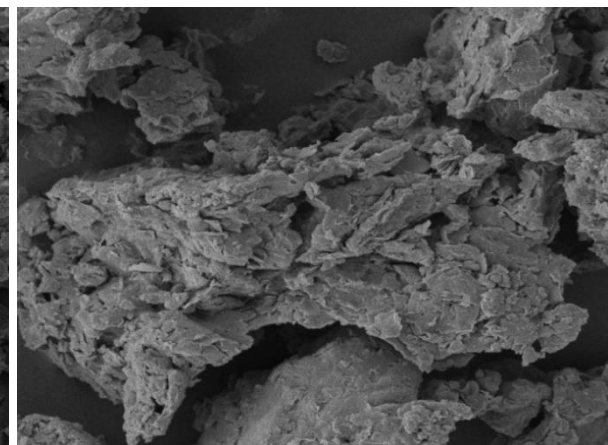
c) GT (Mag: 1500x)



d) GT-pB10 (Mag: 1500x)

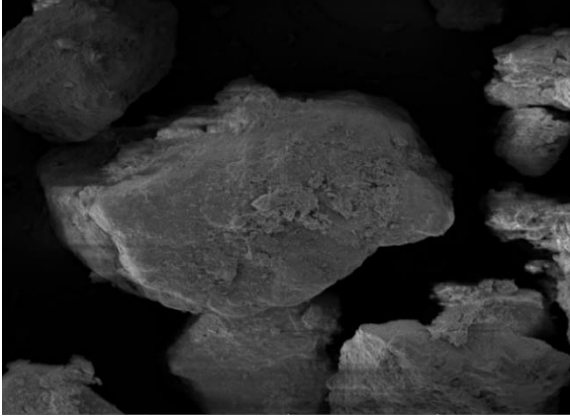


e) GT (Mag: 5000x)



f) GT-pB10 (Mag: 5000x)

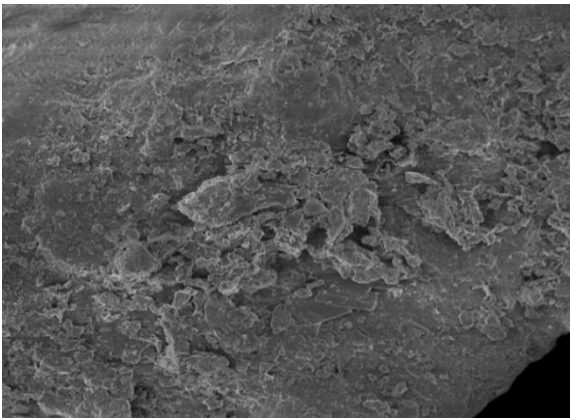
Figure A. 3 SEM image comparison between GT and GT with pPCM-B at different magnification values



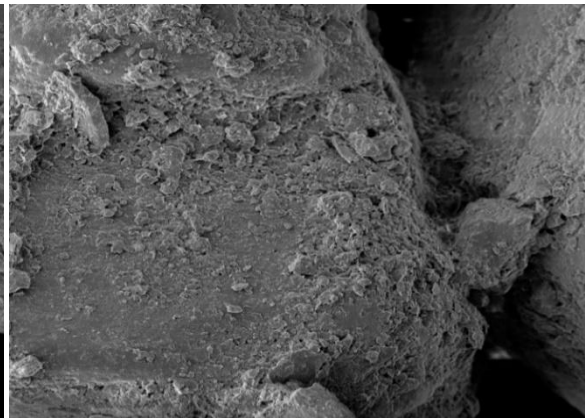
a) SS (Mag: 500x)



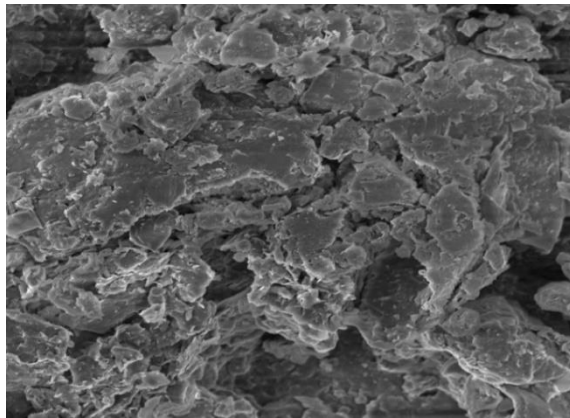
b) SS-A10 (Mag: 500x)



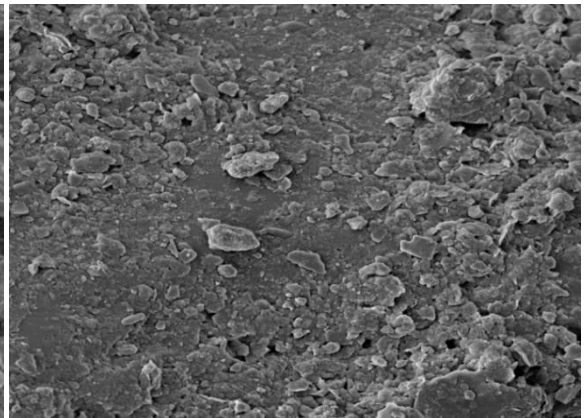
c) SS (Mag: 1000x)



d) SS-A10 (Mag: 1000x)

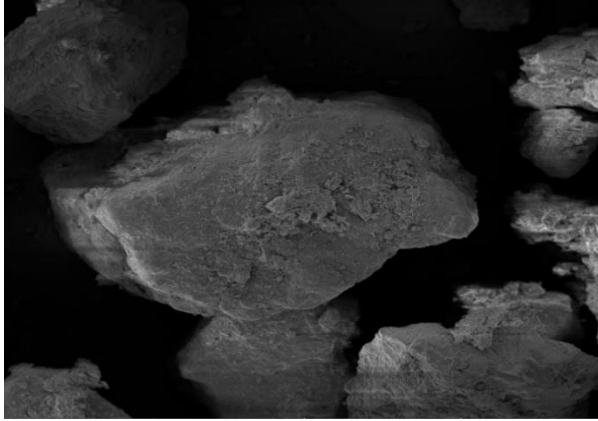


e) SS (Mag: 5000x)

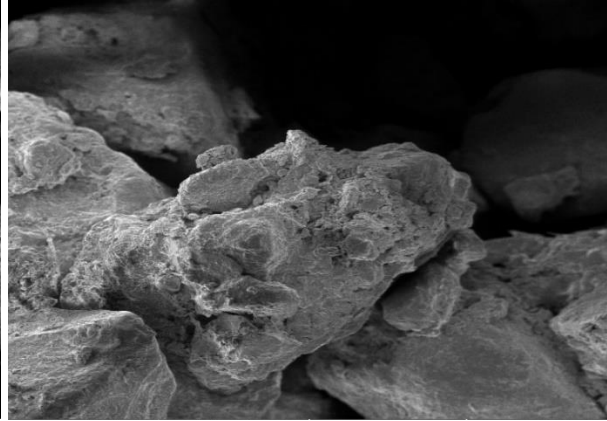


f) SS-A10 (Mag: 5000x)

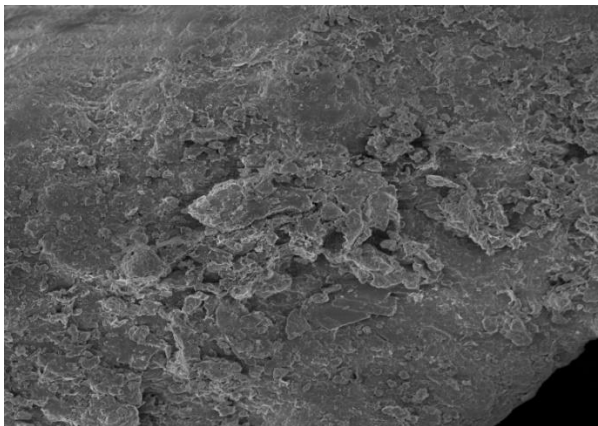
Figure A. 4 SEM image comparison between SS and SS with PCM-A at different magnification values



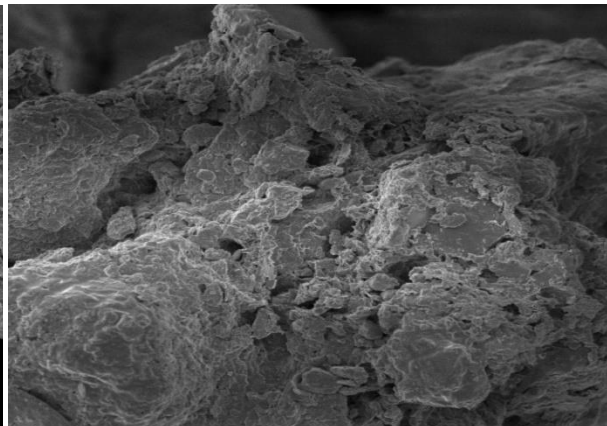
a) SS (Mag: 500x)



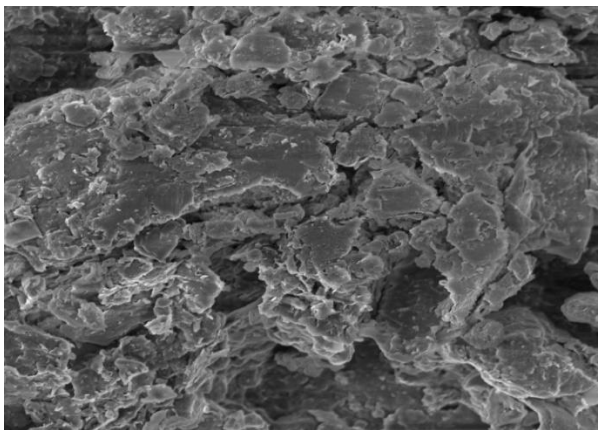
b) SS-B10 (Mag: 500x)



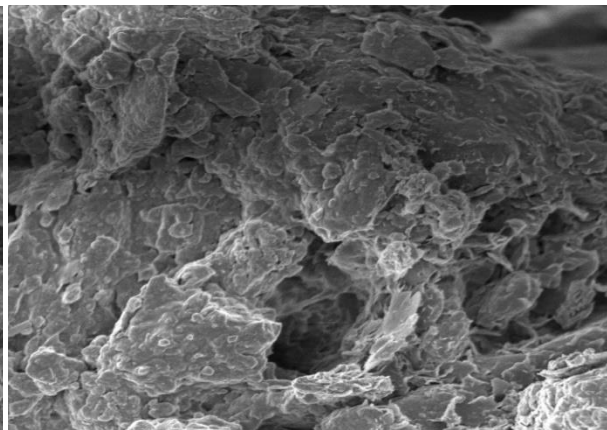
c) SS (Mag: 1000x)



d) SS-B10 (Mag: 1000x)

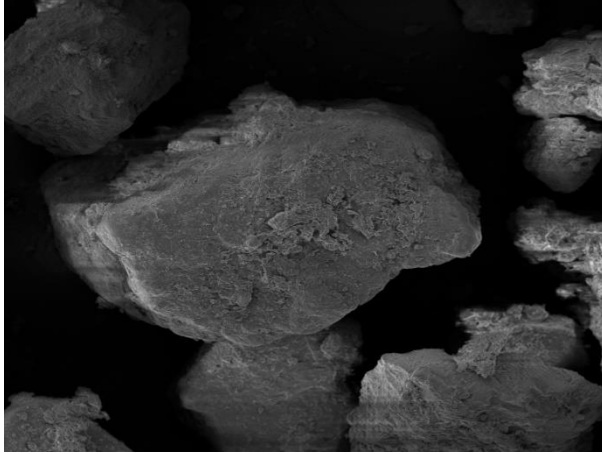


e) SS (Mag: 5000x)



f) SS-B10 (Mag: 5000x)

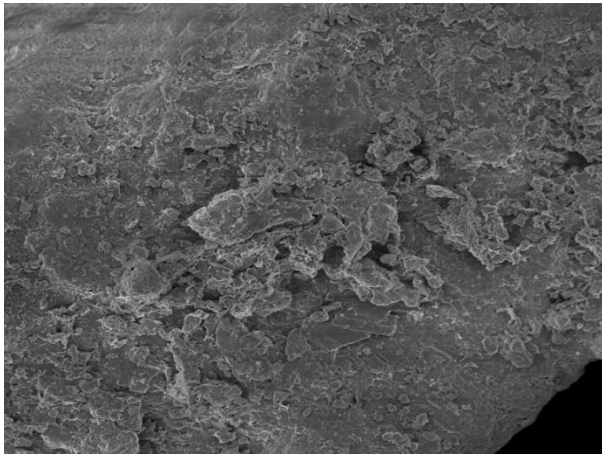
Figure A. 5 SEM image comparison between SS and SS with PCM-B at different magnification values



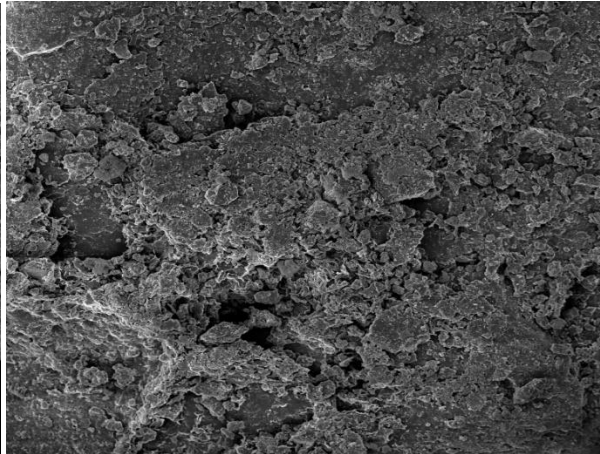
a) SS (Mag: 500x)



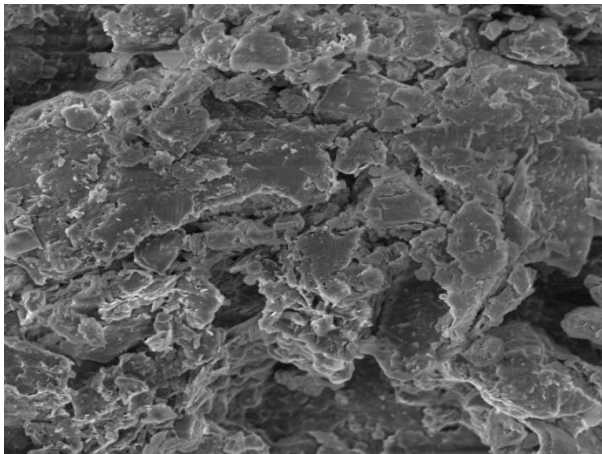
b) SS-pB10 (Mag: 500x)



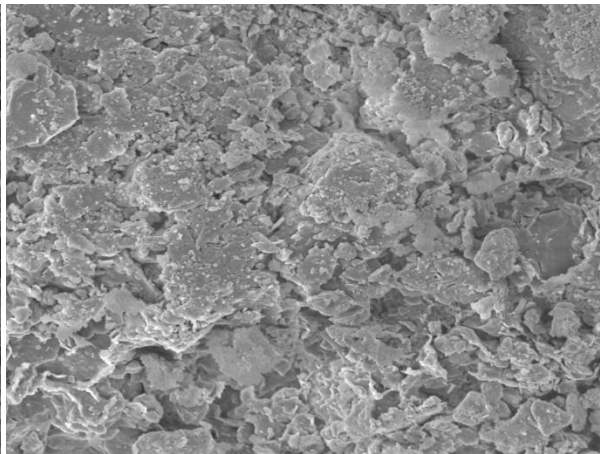
c) SS (Mag: 1000x)



d) SS-pB10 (Mag: 1000x)



e) SS (Mag: 5000x)



b) SS-pB10 (Mag: 5000x)

Figure A. 6 SEM image comparison between SS and SS with pPCM at different magnification values